2014-01-01

An Experimental Investigation on Liquid Methane Heat Transfer Enhancement through the Use of Longitudinal Fins in Cooling Channels

Manuel De Jesus Galvan
University of Texas at El Paso, mjgalvan2@miners.utep.edu

AN EXPERIMENTAL INVESTIGATION ON LIQUID METHANE HEAT TRANSFER ENHANCEMENT THROUGH THE USE OF LONGITUDINAL FINS IN COOLING CHANNELS

MANUEL DE JESUS GALVAN

Department of Mechanical Engineering

APPROVED:

Ahsan Choudhuri, Ph.D., Chair

Vinod Kumar, Ph.D.

Cristian Botez, Ph.D.

Bess Sirmon-Taylor, Ph.D.
Interim Dean of the Graduate School

AN EXPERIMENTAL INVESTIGATION ON LIQUID METHANE HEAT TRANSFER ENHANCEMENT THROUGH THE USE OF LONGITUDINAL FINS IN COOLING CHANNELS

by

MANUEL DE JESUS GALVAN, B.S. Mechanical Engineering

THESIS

Presented to the Faculty of the Graduate School of

The University of Texas at El Paso

in Partial Fulfillment

of the Requirements

for the Degree of

MASTER OF SCIENCE

Department of Mechanical Engineering

THE UNIVERSITY OF TEXAS AT EL PASO

August 2014

Acknowledgements

I would like to thank the faculty and staff of the Mechanical Engineering department at the University of Texas at El Paso. I would also like to acknowledge NASA and the URC team for their support of this research under award No(s) NNX09AV09A. I would also like to acknowledge my advisor Dr. Ahsan Choudhuri from the University of Texas at El Paso and my mentor Dr. John C. Melcher from NASA JSC for giving me direction during the completion of this work.

Abstract

In the past years, hydrocarbon fuels have been the focus of attention as the interest in developing reusable, high-performing liquid rocket engines has grown. Liquid methane (LCH_4) has been of particular interest because of the cost, handling, and storage advantages that it presents when compared to currently used propellants. Deep space exploration requires thrusters that can operate reliably during long-duration missions. One of the challenges in the development of a reliable engine has been providing adequate combustion chamber cooling to prevent engine failure. Regenerative (regen) cooling has presented itself as an appealing option because it provides improved cooling and engine efficiency over other types of cooling, such as film or dump cooling. Due to limited availability of experimental sub-critical liquid methane cooling data for pressure-fed regen engine design, there has been an interest in studying the heat transfer characteristics of the propellant. For this reason, recent experimental studies at the Center for Space Exploration Technology Research (cSETR) at the University of Texas at El Paso (UTEP) have focused on investigating the heat transfer characteristics of sub-critical CH_4 flowing through smooth sub-scale cooling channels. In addition to investigating smooth channels, the cSETR has conducted experiments to investigate the effects of internal longitudinal fins on the heat transfer of methane. To conduct the experiments, the cSETR developed a conduction-based thermal concentrator known as the High Heat Flux Test Facility (HHFTF) in which the channels are heated. In this study, a smooth channel and three channels with longitudinal fins all with cross sectional geometries of 3.2 mm x 3.2 mm were tested. The Nusselt numbers ranged from 70 and 510, and Reynolds numbers were between 50,000 and 128,000. Sub-cooled film-boiling phenomena were discovered in the data pertaining to the smooth and two finned channels. Sub-cooled film-boiling was not observed in the channel that had the fins with the highest height. Film-boiling onset at Critical Heat Flux (CHF) was correlated to a Boiling Number (Bo) of approximately 0.1 for the channels studies. Convective Nusselt number follows predicted trends for Reynolds number with a wall temperature correction factor for both the boiling and non-boiling regimes.

Table of Contents

List of Tables

List of Figures

Chapter 1: Introduction

1.1 Project Overview

Growing interest in space exploration and longer duration missions has led to a need for improving the reliability of propulsion systems. Current propulsion systems generally use liquid hydrogen (LH_2) and liquid oxygen (LOX), as well as monomethylhydrazine (MMH) and nitrogen tetroxide (NTO). One issue with current propulsion systems is the fact that they are expensive due to handling requirements. For example, LOX/LH_2 systems have high production and storage costs due to cryogenic temperature requirements, and MMH and NTO have high handling costs due to the safety precautions that need to be taken due to their toxicity and instability [1]**.** The previously mentioned issues may be resolved with the use of non-toxic propellant systems. One type of non-toxic propellant is liquid methane (LCH_4), which is not only non-toxic, but has similar storage temperature requirements as LOX, which eliminates the need to have different storage tank systems. In addition, LCH_4 has a higher boiling point at ambient conditions (110 K) than LH_2 (20 K), which translates to lower production and storage costs [2**]**. Furthermore, LOX/LCH_4 systems are safer than hypergolic propellants such as MMH and NTO, which are toxic and corrosive. LCH_4 is also an attractive propellant because it may be produced on other astronomical bodies via In Situ Resource Utilization (ISRU).

Currently, LOX/LCH_4 systems are being researched to develop thrusters that are reliable for deep space exploration and long-duration missions. One of the challenges in the development of such an engine has been providing adequate combustion chamber cooling to prevent engine failure. Common cooling methods include film cooling, ablative cooling, dump cooling, and regenerative cooling [3]. Regenerative (regen) cooling has presented itself as an appealing option because of its advantages over other types of cooling. For example, regen engines offer improved cooling and higher engine efficiency because these types of engines use fuel to cool the engine by flowing the fuel along the nozzle and combustion chamber walls through cooling channels before being injected into the combustion chamber and being combusted to provide thrust. In film or dump cooling, the fuel used as a coolant is not combusted; therefore, the fuel does not provide thrust, and it simply exits the engine after cooling the walls, whereas regen engines take advantage of the fuel being used as the coolant to provide thrust.

Currently, NASA Johnson Space Center (JSC) is developing an autonomous vehicle designed to test lander technologies [4].

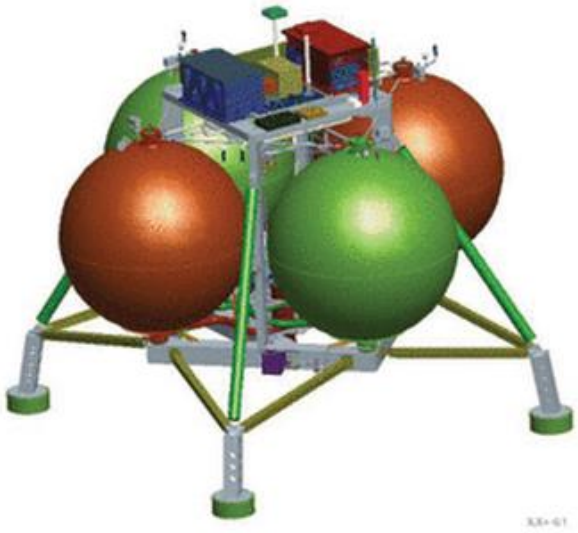

Figure 1.1: Model of Morpheus, a Lander Vehicle Developed by NASA [4].

This lander vehicle, known as the Morpheus vehicle, incorporates a LOX/LCH_4 blowdown propellant system in which system pressures remain subcritical. Figure 1.1 shows a model of the Morpheus vehicle. Furthermore, NASA is developing a regen LOX/LCH_4 engine for the Morpheus vehicle; however, a design challenge regarding regeneratively-cooled rocket engines is the fact that there is limited empirical data for subcritical methane heat transfer. Due to the growing interest of liquid methane (LCH_4) use as a propellant in lander class space vehicle engines, the High Heat Flux Test Facility (HHFTF) was developed at the Center for Space Exploration Technology Research (cSETR) to provide empirical LCH_4 data by investigating the behavior of LCH_4 flowing through subscale single channel test articles.

1.2 Project Objectives

The purpose of this study is to experimentally investigate the heat transfer characteristics of subcritical methane using single channel test articles at steady state conditions. Such conditions include heat flux, bulk properties, and channel wall temperatures. During the investigation, the study will focus on observing the effects of longitudinal fins machined in cooling channels on the cooling behavior of

subcritical methane. The study will achieve this by exposing the cooling channels to conditions present in a regen engine. Three channels with internal longitudinal fins of different heights were machined to compare the cooling performance of the fin-enhanced channels to the performance of a smooth channel. The channels used in the investigation have an identical cross-sectional geometry, with the exception of the longitudinal fins, so that the performance may be fairly compared. It is expected that the cooling performance will increase with increasing fin height, but at the expense of increased pressure drops within the channels.

1.3 Experimental Approach

To understand the behavior of hydrocarbon propellants under conditions encountered in rocket engines, several facilities that subject the hydrocarbons to high heat fluxes have been developed. These heat flux facilities employ combustion, arc lamp, laser, conductive, and resistive heating to replicate the heat fluxes encountered in rocket engines [5]. Recent studies have focused on conductive and resistive heating due to their practicality when compared to other types of heating. Of these two types of heating, conduction heating was chosen to provide a constant heat flux to the cooling channel test articles due to the advantages that conduction heating has over resistive heating; one such advantage is the fact that a conductively heated facility will heat a test article asymmetrically, which is what a cooling channel on a regeneratively-cooled engine will is subjected to during engine operation. The cSETR HHFTF is supplied with liquid methane via a 13 L condenser that was developed at the cSETR. At lander class engine conditions, the condenser can successfully provide enough methane to be able to obtain steady state conditions.

1.4 Relevance

With the data collected from the experiment, it will be attempted to gain an understanding of the heat transfer characteristics of subcritical LCH_4 and the effects that longitudinal fins impose on the behavior via heat transfer enhancement. In addition, the study presents the effects that fins have on boiling phenomena within a channel, which may be used as the basis for designing a study that further investigates the effects of longitudinal fins on boiling phenomena within cooling channels. With additional testing, it will be possible to develop Nusselt number (Nu) correlations to predict heat transfer

coefficients and facilitate designers' attempts to develop an engine that will be effectively cooled. Furthermore, the results of the experiment will provide a basis for comparison for CFD simulations performed involving liquid methane. Overall, the results from the experiment will provide a foundation for the design of cooling channels involving subcritical LCH_4,which will be of great importance to the aerospace industry.

Chapter 2: Literature Review

2.1 High Heat Flux Facilities

The need for liquid methane convective heat transfer data spawned an interest in the development of a test rig that replicates the conditions that a propellant is subjected to in regeneratively cooled rocket engine cooling channels. An exemplary test setup accurately simulates wall temperatures, pressures, and heat fluxes observed in regenerative engine cooling channels to study the thermal behavior of fuels as coolants. Furthermore, a desirable test rig allows for ample instrumentation while being overall relatively low cost. High heat flux facilities are an attractive option that allow the study of hydrocarbon fuel convective heat transfer, fuel and channel wall material compatibility, and coking limits by implementing the use of instrumented subscale cooling channels subjected to a heat flux, all while having a lower cost than an actual regenerative engine. To reach the high temperatures needed to investigate the behavior of hydrocarbon fuels at conditions present in combustion chamber cooling channels, high heat flux facilities may make use of one of several ways to heat the subscale channel. More specifically, a high heat flux facility may use resistive or conductive heating to subject the subscale cooling channels to a desired heat flux [6].

2.1.1 Resistively Heated Tubes

High heat flux facilities that make use of electrical resistance to generate heat by passing current through a metal tube are referred to as resistively heated tube facilities [6]. Some examples of resistively heated tube facilities include the NASA-Glenn Research Center Heated Tube Facility and the NASA-Marshall Space Flight Center/Rocketdyne Electrically-Heated Tubular Test Specimen, which studied the cooling capability, coking threshold, and the fuel's thermal stability [5**,** 7]. Furthermore, a resistively heated tube facility was developed at Xi'an Jiaotong University to study the convective heat transfer of methane [8]. While resistively heated tube facilities allow for more precise control of heat flux applied to a specimen, the high currents needed to raise the test specimen wall temperature cause electrically driven chemical phenomena, which may negatively affect the data obtained [9].

NASA-Glenn Research Center

In 2010, the NASA Glenn Research Center Heated Tube Facility (HTF) used resistive heating to generate the high wall temperatures needed to simulate the conditions observed in regeneratively cooled rocket engine cooling channels. The test sections used in the study were constructed of Inconel 600 and had nominal inner diameters of 0.57-, 1.37-, and 1.91-mm, and were 368 mm in length. The tubes were heated by passing a current through the cooling channel; currents of up to 1500 A were used to heat the tubes using a 100 VDC power supply, and average heat fluxes of 10.1 MW/m^2 were reached. The test section under study was placed vertically inside of a vacuum chamber as shown in Figure 2.1 to reduce convective losses, which allows for more accurate heat transfer calculations, and to contain the setup in the event of a test section failure or fuel leak [10]. The tubes were used to investigate the cooling characteristics of subcooled methane flowing at rates between 2.3 to 31.8 g/s at inlet pressures as high as 5.5 MPa; the temperature range of subcooled methane ranged from 104 to 142 K.

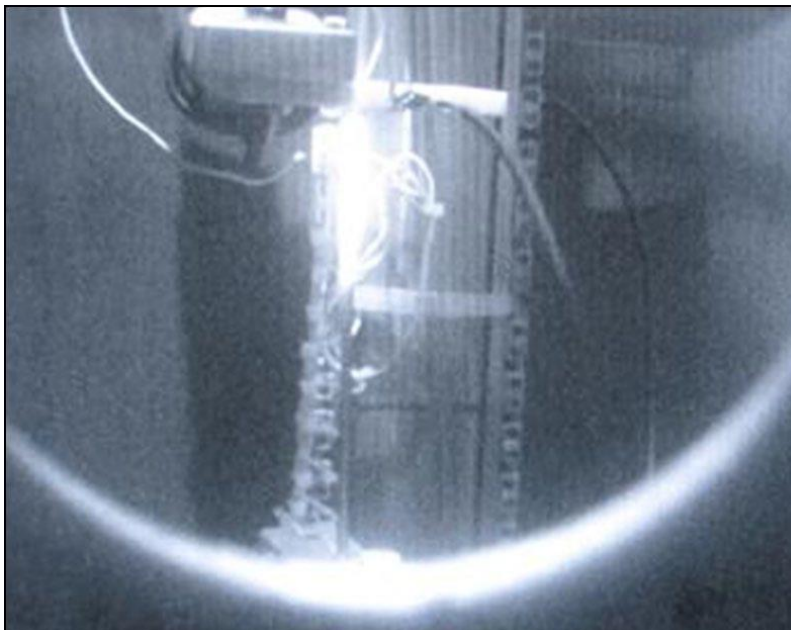

Figure 2.1: Image of Test Sample Placed in Vacuum During a Test [10]

United Aircraft Corporation, Pratt and Whitney Aircraft Division

The 1967 study was conducted to study the heat transfer characteristics as well as the nucleate and film boiling during internal forced convection flow of several hydrocarbon fuels [11]. The hydrocarbons that were studied include methane, propane, propylene, butene-1, and other hydrocarbon blends. The study used a resistively heated 990 mm long test section made of Inconel 600 having an outer diameter of 9.5 mm and wall thickness of 0.4 mm to study boiling phenomenon of the mentioned hydrocarbons. The test section was placed in a vacuum chamber to reduce convective losses, and the inlet chamber was insulated from connecting plumbing to minimize conductive losses. The wall temperatures were measured with 16 type K thermocouples spot-welded to the outer tube surface of the heated tube section, which was 838 mm long. Tests were conducted at the hydrocarbons' normal boiling point to the triple point, and pressures ranged from 1/3 to 1.2 times the hydrocarbons' critical pressures.

NASA-Marshall Space Flight Center/Rocketdyne

The NASA Marshall Space Flight Center (MSFC)/Rocketdyne test facility was used to study the coking thresholds of methane and to develop convective correlations for the heat transfer characteristics of the hydrocarbon in 1984. The Rocketdyne test facility made use of electrically heated tubes to replicate conditions similar to those observed in the main combustion chamber cooling channels in the Space Shuttle Main Engine (SSME); furthermore, the study sought to provide an understanding of the coking threshold and heat transfer data of methane flowing through copper channels. The cooling channels used to test higher heat fluxes were 178 mm in length, while the cooling channels used to test lower heat flux conditions were 76 mm in length. The channels had an inner diameter of 1.85 mm and outer diameter of 2.62 mm. Figures 2.1 and 2.2 show the test section assembly and thermocouple placement on the heated sections of the tube.

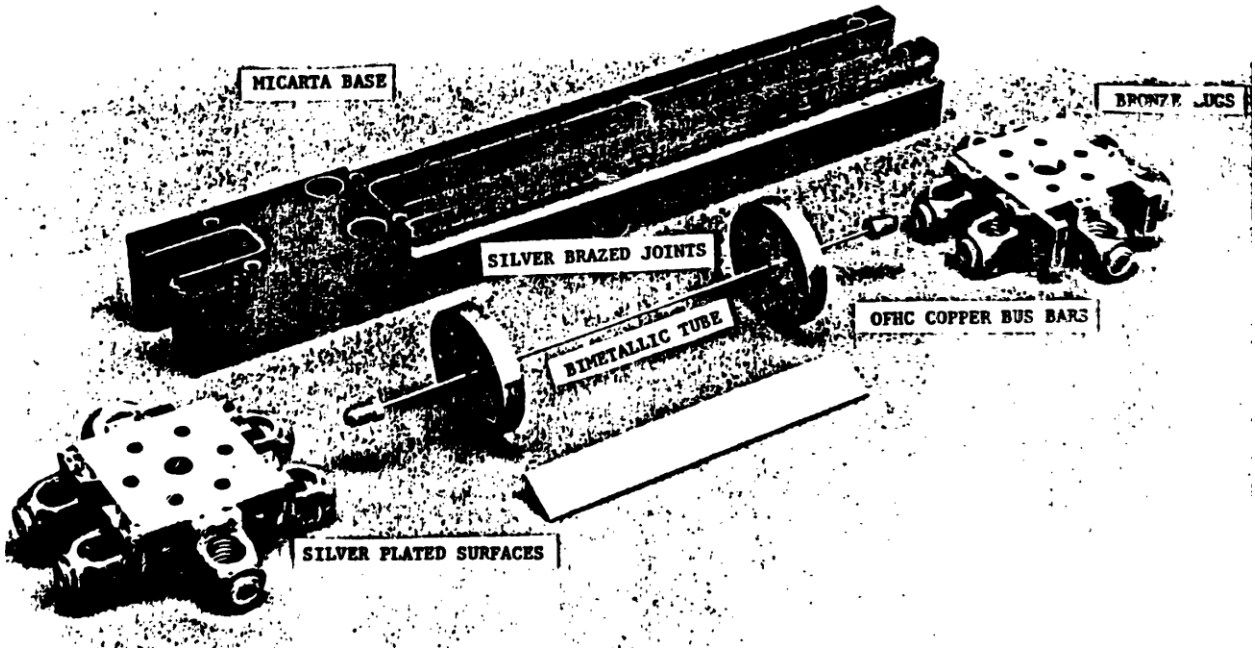

Figure 2.2: MSFC-Rocketdyne Test Section Assembly [7]

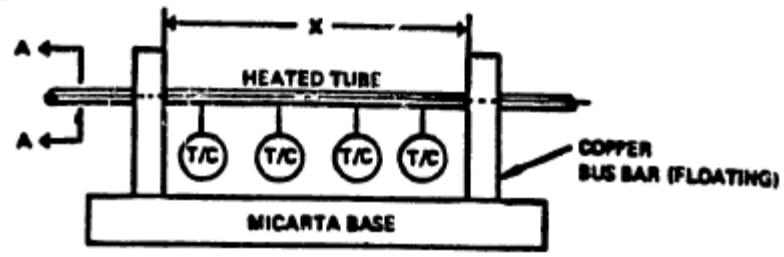

Figure 2.3: MSFC-Rocketdyne Thermocouple Placement on Heated Sections of Tube [7]

To simulate the conditions reached during engine operation, the Rocketdyne test facility used three arc reactors rated at 2000 A each. The specific engine operating conditions that were replicated were heat fluxes of up to 139 MW/m^2, wall temperatures ranging from 316 °C to 482 °C, working fluid pressures as high as 31 MPa, and fluid velocities ranging from 55.2 to 238.0 m/s. The fluid flow rate was controlled by the tank pressure and a downstream valve [7].

Xi'an Jiaotong University

When compared to supercritical studies of substances such as carbon dioxide, water, kerosene, and other substances, there are limited supercritical methane heat transfer studies in literature. To provide heat transfer data of methane at supercritical pressures, Hongfang et al. developed an

experiment at Xi'an Jiaotong University to study the convective heat transfer of cryogenic methane [8]. This was achieved in 2013 by flowing methane through a miniature stainless steel circular tube that allowed the methane to be studied at pressures of up to 20 MPa and to be subjected to heat fluxes as high as 25 MW/m^2. The test sections used were 200 mm in length and 2.6 mm in diameter; furthermore, they were constructed of 1Cr18Ni9Ti stainless steel, and had wall thicknesses of 0.5 mm. The tubes were heated electrically with AC power supplies having an output of 100 kW, and the wall temperature was adjusted by controlling the electric current applied to the tubes. Wall temperatures were measured using type K thermocouples soldered to the tubes' outer wall, and channel pressures were monitored with two pressure transducers placed at the inlet and outlet of the tube. Figure 2.4 shows the thermocouple and power supply electrode placement on the test section. The methane was pressurized by a low-temperature pump to pressures of up to 28 MPa, which yielded flow rates as high as 1.5 m^3/h. The conditions studied in the experiment were inlet pressures ranging from 5 to 15 MPa, and heat fluxes ranging from 1 to 16 MW/m^2 [8].

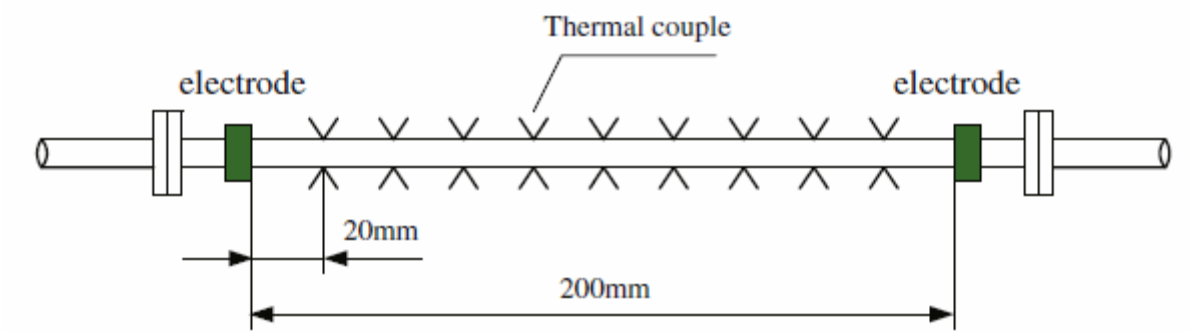

Figure 2.4: Thermocouple and Power Supply Electrode Placement on Test Section [8]

2.1.2 Conductively Heated Tubes

Facilities that use conductive heating to supply a heat flux to test specimens are known as conductively heated tube facilities. The Aerojet Carbothermal test rig, is an example of a conductively heated facility, which was developed to identify corrosive interactions between hydrocarbon fuels and combustion chamber materials, as well as to propose possible solutions to eliminate the degradation of the chamber wall materials [12]. Another conductively heated test facility is the Air Force Research Laboratory High Heat Flux Facility (HHFF), which was based on the Aerojet Carbothermal Rig. The

HHFF was designed as an extension of the Aerojet Carbothermal Rig to generate heat fluxes higher than those achieved with the Aerojet test facility [9]. Overall, conductively heated tubes better replicate the conditions present in a regeneratively cooled rocket engine combustion chamber cooling channel, one of which is asymmetric heating, without introducing chemical phenomena caused by high currents like the ones used in resistively heated test facilities.

Aerojet Carbothermal Rig

In 1990, the Aerojet Carbothermal Rig study made use of conduction heating to focus a heat flux onto a test section; a large copper block embedded with cartridge heaters provided the heat input to the channel being studied. The cartridge heaters heated the copper block to a desired temperature, and the block conductively heated the small test section with a channel milled into it by geometrically focusing its thermal energy onto the test section [5]. Figure 2.5 shows the Carbothermal Rig's test section and heating block layout [12].

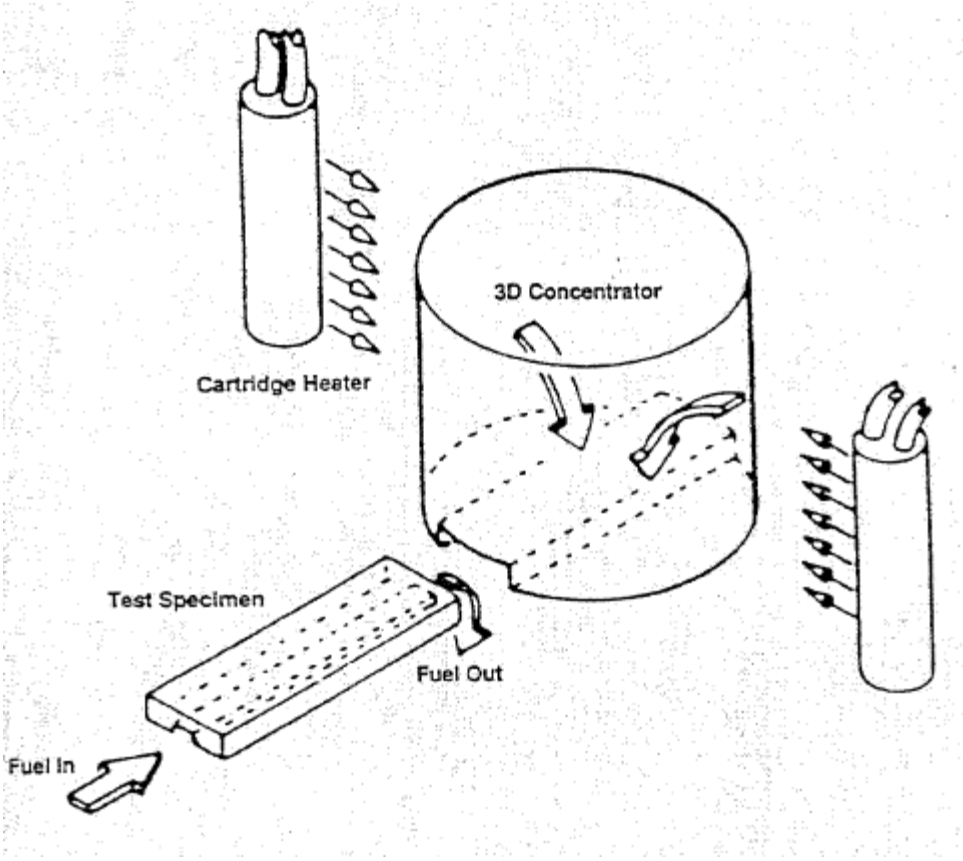

Figure 2.5: Carbothermal Rig Test Section and Heating Block Layout [12]

The Carbothermal Rig was used to study hydrocarbon fuel and copper chamber liner material compatibility; more specifically, the test facility employed static and dynamic test methods to determine fuel/liner material compatibility. Static tests consisted of exposing copper sample pieces to fuel for long durations at constant temperature and pressure, while dynamic tests made use of the Carbothermal Rig to simulate heat fluxes, wall temperatures, and pressures expected in a regeneratively cooled rocket engine combustion chamber [12]. Pressures of up to 24.1 MPa and heat fluxes as high as 86.7 MW/m^2 were studied using hydrocarbon fuels such as methane, propane, and RP-1 [5, 9].

Air Force Research Laboratory High Heat Flux Facility (HHFF)

With the growing interest in reusable liquid hydrocarbon-fueled rocket engines, it became necessary to develop a way to test the cooling characteristics of hydrocarbon fuels flowing through subscale cooling channels and the compatibility of such fuels with combustion chamber wall materials. The hydrocarbon fuel that the Air Force Research Laboratory HHFF focused on was RP-2 fuel [5, 9, 13, 14]. The HHFF went through several design iterations to develop a heating block that would provide both heat flux and temperature uniformity within the test section. The chosen design combined previous design iterations to present a block that would provide improved thermal performance; more specifically, the chosen design combined asymmetric heating with geometric focusing from the first design to heat the test section, which improved upper test section wall uniformity due to faster thermal replenishment, as well as the embedding of the test section in the heater block from a later design iteration, which brought the heating block's thermal mass closer to the test section [13], as shown in Figure 2.6.

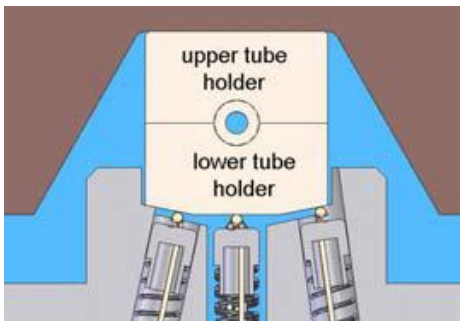

Figure 2.6: High Heat Flux Facility Original Cradle Design [13]

An additional benefit of the test facility design was the fact that changing the cooling channel geometry was as simple as replacing the test section, and not the whole heating block, which would have been the case with a previous design [5, 9]. To reduce convective losses and reduce oxidation of the equipment, the test section and block were placed inside an altitude chamber. The reduction of convective losses inside the vacuum chamber also allowed more accurate heat transfer calculations. Overall, the HHFF design accurately simulated the conditions in a regeneratively cooled rocket engine, namely pressures of up to 31.0 MPa and wall temperatures of up to 650 °C by supplying a heat flux of 163.5 MW/m^2 [5, 9].

To further improve the heat transfer and alignment of the test section and heating block, the original HHFF rig design was modified to incorporate a different cradle configuration. In the original cradle design, the cooling channel and test section were separate from the heating block, with the heating block coming into contact with the upper surface of the upper tube holder block, as shown in Figure 2.6 [13]. In the modified test section/block design, the upper tube holder was eliminated [13], and a groove in the shape of the cooling channel was machined into the heating block as shown in Figure 2.7.

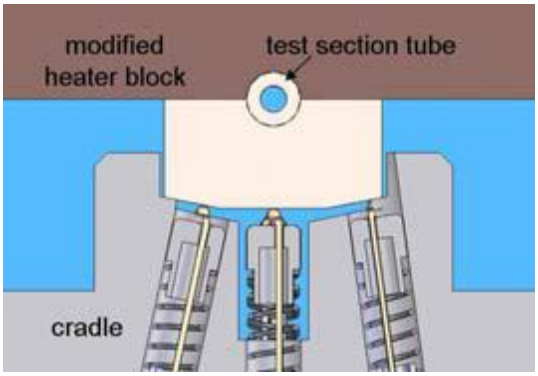

Figure 2.7: High Heat Flux Facility Modified Cradle Test Section Design [13]

2.2 Liquid Methane Heat Transfer Studies

To develop liquid oxygen/liquid methane thrusters that provide higher performance when compared to similarly sized propellant systems, cooling data on liquid methane is necessary. Due to the limited amount of cooling data available, several studies have been developed to investigate the heat

transfer of liquid methane and provide data for proper regenerative engine design. The following studies present cooling data for both subcritical and supercritical methane.

NASA Glenn Research Center

In 2010 the Propulsion and Cryogenic Advanced Development (PCAD) project at NASA Glen Research Center ran a series of tests to investigate the heat transfer of liquid and two-phase subcritical methane. More specifically, the series of tests sought to develop heat transfer correlations for liquid methane. Another objective of the PCAD project was to measure system pressure drops in the two-phase regime; however, the key objective was to determine the critical heat flux for a given set of conditions [10].

To study the heat transfer of liquid methane, the PCAD project used a Heated Tube Facility (HTF) that was developed to simulate heat flux conditions in a regeneratively cooled rocket engine [15]. A test consisted of flowing liquid methane through the facility's resistively heated tube until the channel reached a steady state temperature. After reaching a steady temperature, the power supplies are enabled to provide the sample with a heat flux. While maintaining a constant flow velocity, the heat flux applied to the sample was gradually increased to observe the sample's reaction. When the critical heat flux was reached, a point close to the end of the tube undergoes a sudden increase in temperature, usually in the range of 110 to 165 °C per second. The sharp increase in temperature may be observed in Figure 2.8, which shows the temperature of the thermocouple that was placed furthest downstream of the heated section and the heat flux applied to the sample.

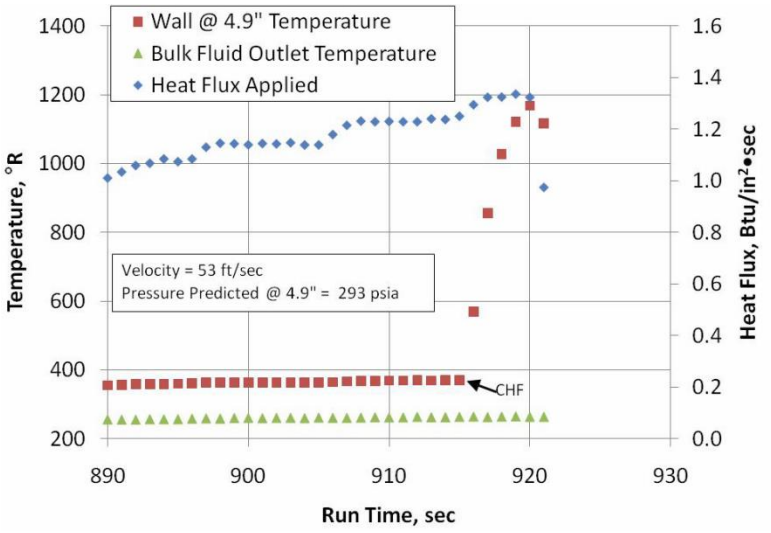

Figure 2.8: Temperatures and Heat Flux Observed Upon Reaching Critical Heat Flux [10]

It was found that the change from nucleate to film boiling was more discernible for test section pressures below 2.07 MPa; for pressures above 3.1 MPa, the transition from nucleate to film boiling was not as obvious.

United Aircraft Corporation, Pratt and Whitney Aircraft Division

The study conducted by Glickstein and Whitesides in 1967 yielded approximately 500 tests for six hydrocarbons, with most tests being conducted at supercritical pressures. The tests allowed data on nucleate and film boiling at subcritical pressures to be obtained, as well as maximum nucleate boiling heat fluxes, film boiling coefficients, and forced convection film coefficients at supercritical pressures. Figure 2.9 shows the typical wall temperature profile for subcritical methane boiling in the heated tube.

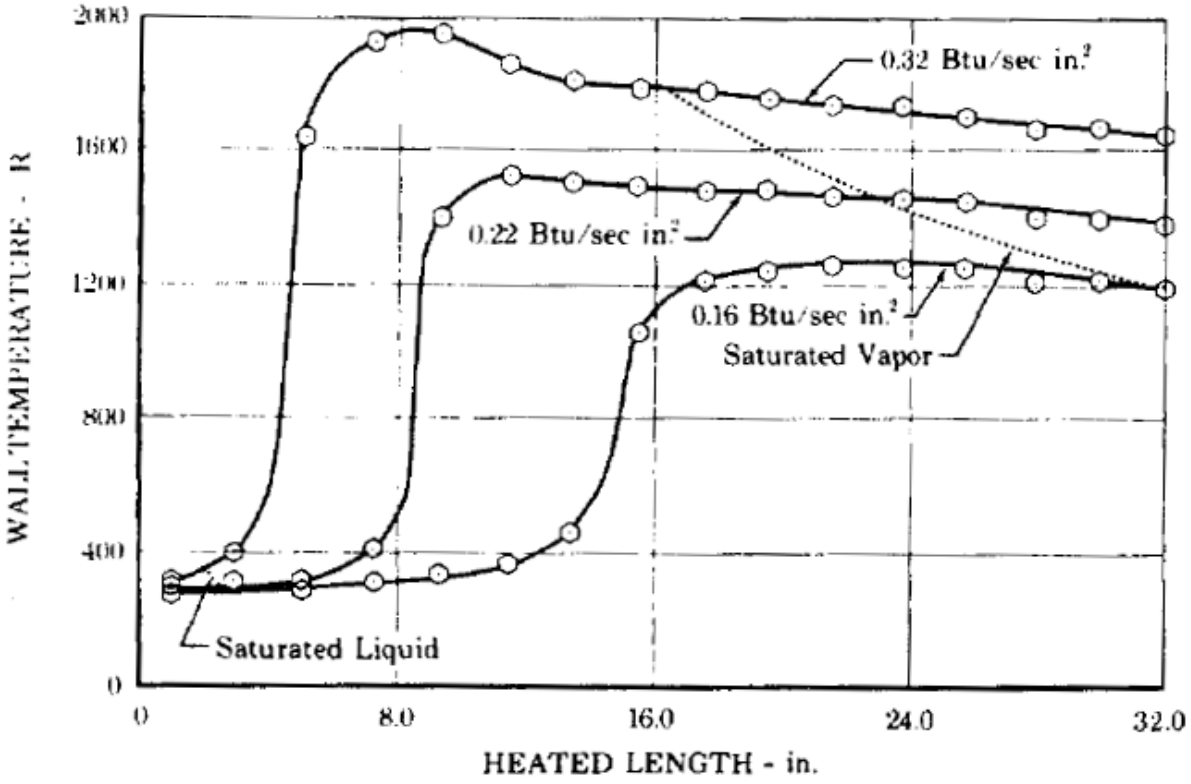

Figure 2.9: Typical Wall Temperature Profile for Subcritical Methane [11]

At the inlet, wall temperatures are slightly above saturation temperature, which suggests that the methane is in the nucleate boiling region. Past this region, there is a rapid increase in temperature, which is the transition between nucleate and film boiling. It was noted that as the applied heat flux was increased, the transition from nucleate to film boiling shifted towards the inlet, and the maximum wall temperature increased [11].

NASA Marshall Space Flight Center/Rocketdyne

The 12-month program developed in 1984 to investigate the compatibility of methane with copper at high heat fluxes, as well as the thermal decomposition and cooling characteristics of methane in copper cooling channels consisted of 37 tests and a total of 450 data points. The results of the study showed that higher wall temperatures and heat fluxes resulted in increased chemical corrosion at the copper wall. Furthermore, the results showed that high tube wall roughness yielded large increases in pressure drop and heat transfer. Figure 2.10 shows the higher Nusselt numbers for rough tubes when compared to smooth tubes [7].

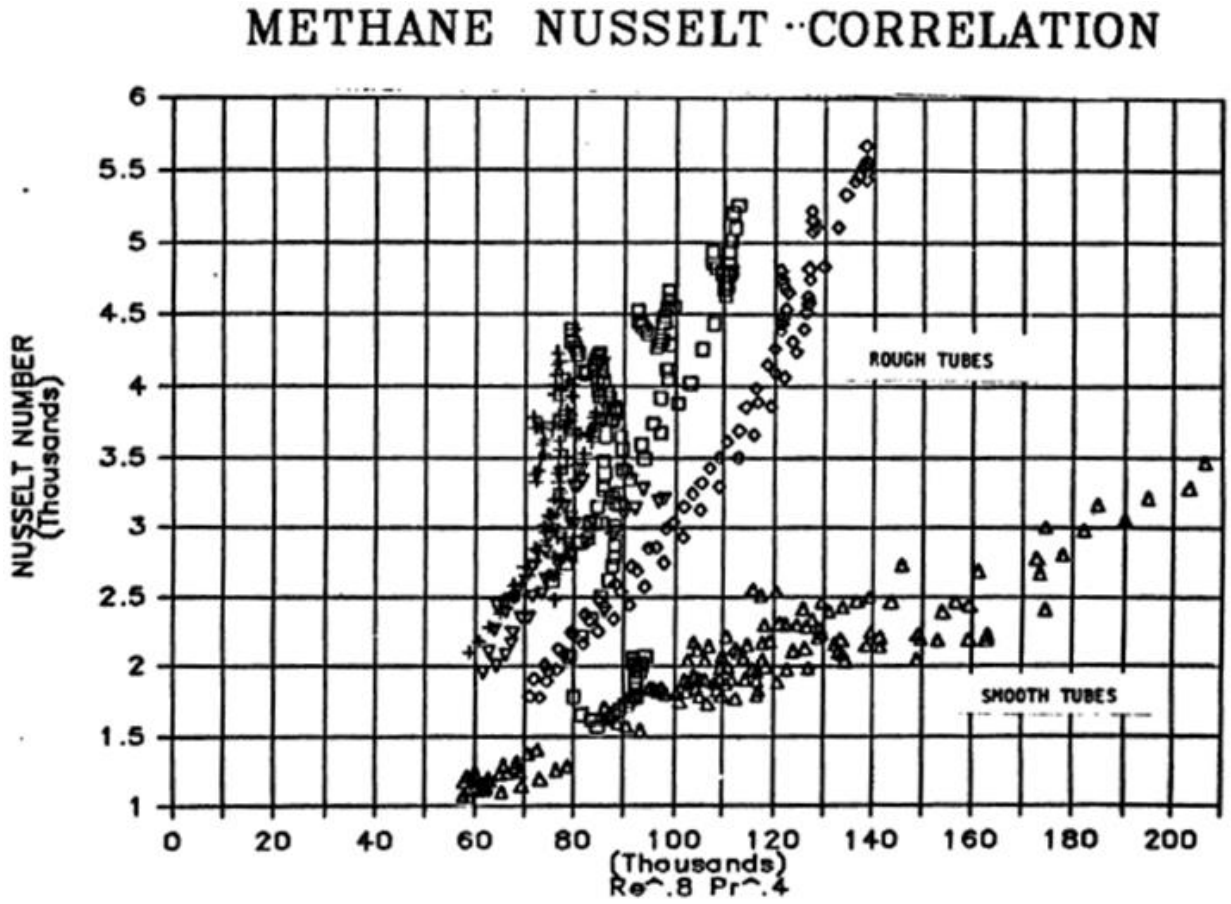

Figure 2.10: Comparison of Nusselt Numbers Obtained Using Rough and Smooth Tubes [7]

Regarding chemical corrosion and coking at the tube copper walls, it was found that there was significant sulfidation, as well as roughening and discoloration in tubes that had liquefied natural gas flowed through them; however, no significant coking was detected.

Xi'an Jiaotong University

Due to drastic property variations near the pseudo-critical temperature, which is the temperature at which the specific heat of a substance is greatest for a given pressure, the study had a particular interest in studying the heat transfer of methane near the pseudo-critical temperature. Ultimately, the results from the experiment would be used to develop a heat transfer correlation for methane at supercritical pressures. To better compare the experimental data at different conditions, the experimental local heat transfer coefficients were normalized by using the Dittus-Boelter correlation evaluated at a pressure of 10 MPa, temperature of -150 °C, and mass flux of 11,000 kg/m^2 s. In addition, the bulk and

wall temperatures were normalized by the pseudo-critical temperature at the inlet temperature. To develop the heat transfer correlation for the cryogenic methane at supercritical pressures, the Dittus-Boelter and Gnielinski correlations were used as the comparison for the experimental data. It was found that the Dittus-Boelter correlation captured 73% of the data with an accuracy of 25%, while the Gnielinski correlation captured 75% of data with an accuracy of 25%. However, both correlations over predicted measurements near the pseudo-critical temperature region due to their sensitivity to the variations of thermophysical properties, as shown in Figures 2.11 and 2.12. To provide a correlation that accounts for the dependency of the fluid properties at instantaneous turbulent temperature, Probability Density Function (PDF)-based properties were proposed. The proposed PDF correlations captured 85% of the experimental data within an accuracy of 25% [8].

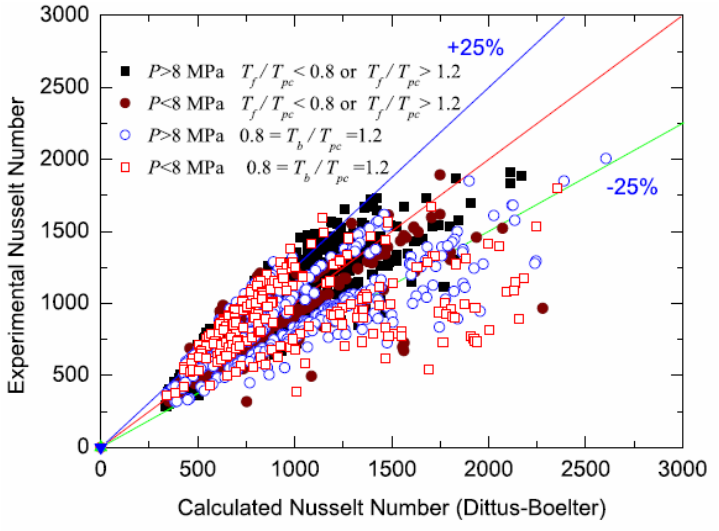

Figure 2.11: Over Prediction of Data Using Dittus-Boelter Correlation [8]

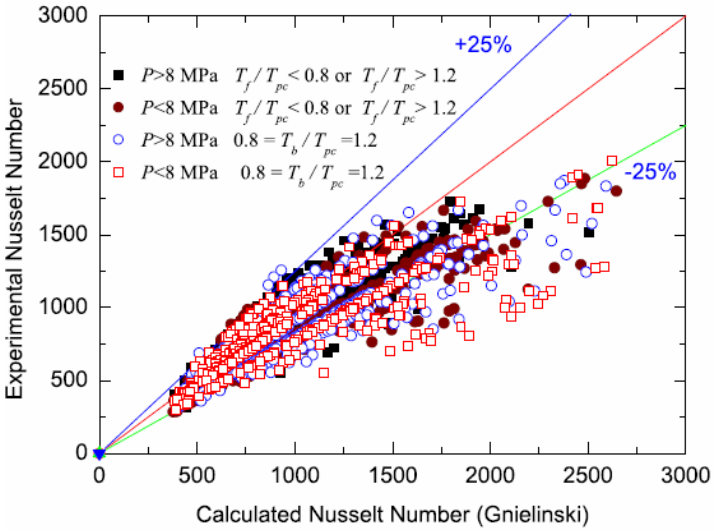

Figure 2.12: Over Prediction of Data Using Gnielinski Correlation [8]

Center for Space Exploration Technology Research- University of Texas at El Paso

In 2013, the Center for Space Exploration Technology Research (cSETR) at the University of Texas at El Paso (UTEP) made use of a high heat flux facility to test the cooling characteristics of a square 1.78 mm x 1.78 mm subscale cooling channel fabricated at NASA's White Sands Test Facility (WSTF). Reynolds numbers obtained ranged from 20000 to 140000, and measured Nusselt numbers ranged from 20 to 260. The measured data points were compared with the correlation presented in the 1984 NASA-Rocketdyne study. Figure 2.13 shows the measured data points compared to the correlation mentioned [16].

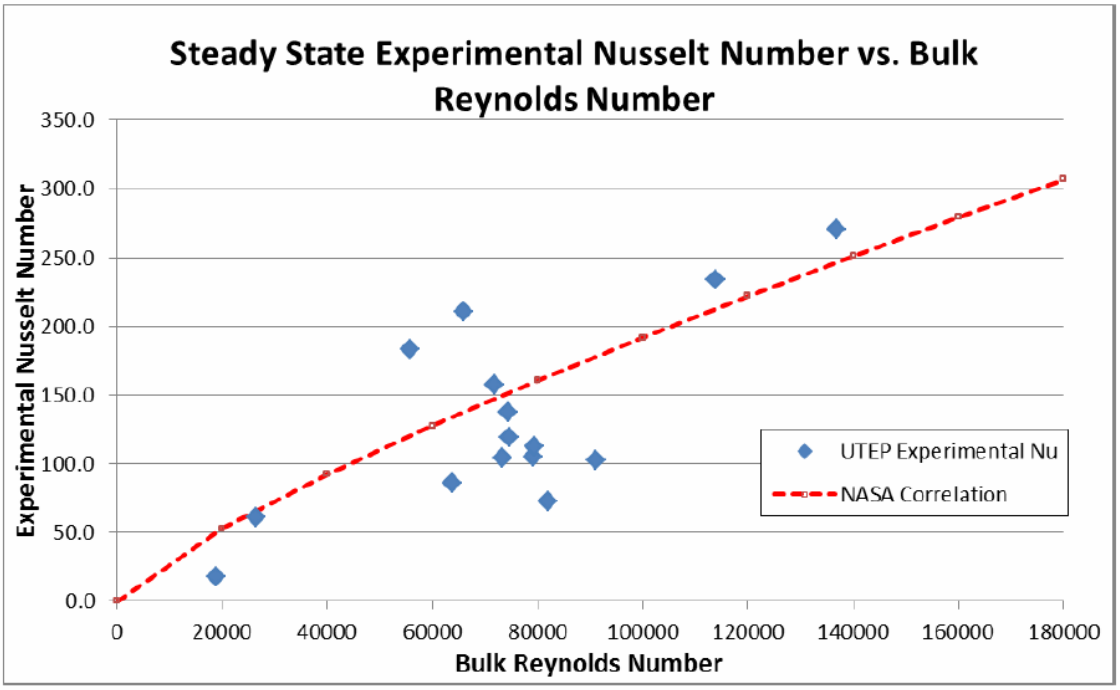

Figure 2.13: Comparison of Measured Data to NASA-Rocketdyne Correlation [16]

Following the investigation of the behavior of liquid methane flowing through the square subscale cooling channel, the cSETR investigated the steady state behavior of liquid methane flowing through subscale cooling channels of different cross-sectional geometries. Channels with different cross-sectional geometries were compared in the 2014 study to observe the effects of channel geometry on heat transfer. The geometries studied include a 1.8 mm x 4.1 mm rectangular channel, a 1.8 mm x 14.2 mm high aspect ratio rectangular channel, a circular channel with interior diameter of 3.18 mm, and a circular channel with interior diameter of 6.35 mm. For the 3.18 mm circular channel studied, a Nusselt number correlation developed by Klimenko [17] for two-phase fluid flow showed the best agreement with the data points [18]. Figure 2.14 shows the high coefficient of determination, R^2, of the correlation.

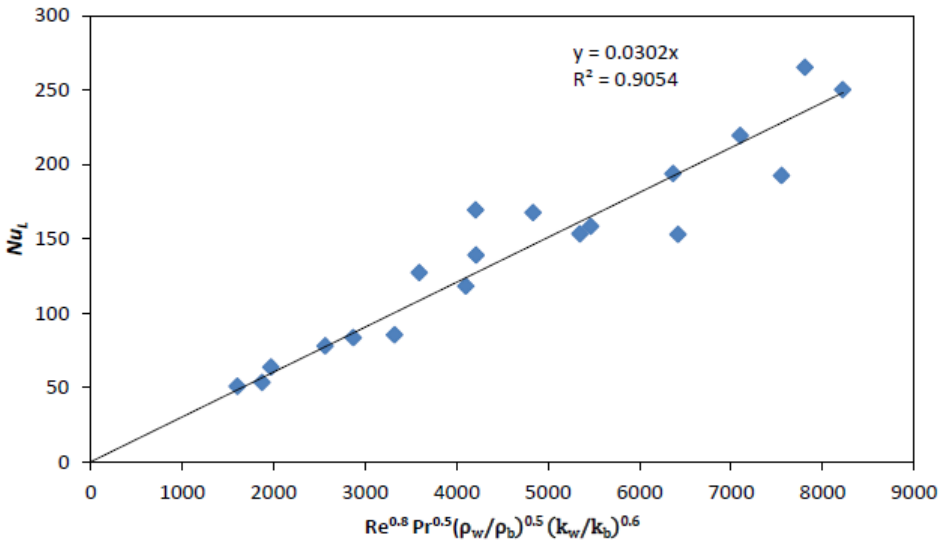

Figure 2.14: Agreement of Klimenko Correlation to Obtained Data [18]

Heat Transfer Enhancements

Heat transfer augmentation techniques are used in heat exchangers used in evaporators, thermal power plants, refrigerator, radiators, and other industries. Two techniques, namely, active and passive, are used to increase heat transfer. Passive techniques are advantageous compared to active techniques because passive techniques use inserts to disturb the flow and increase heat transfer, whereas active techniques require some sort of external energy input. Examples of heat transfer augmentation techniques include twisted tapes, wire coils, ribs, fins, dimpled tubes, and artificial surface roughness. Figure 2.15 shows an example of twisted tape inserts and wire coils.

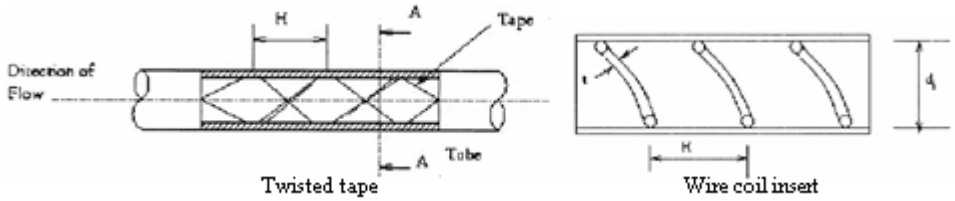

Figure 2.15: Twisted Tape and Wire Coil Inserts [19]

Of the passive heat transfer augmentation techniques, wire coil inserts are more effective in turbulent flow when compared to twisted tapes, because wire coils mix the flow in the viscous sublayer near the wall, whereas twisted tapes do not achieve this. Therefore, twisted tapes are preferred in

laminar flow. Overall, other types of heat transfer augmentation techniques such as ribs, fins, dimpled tubes, and artificially induced roughness are more efficient in turbulent flow than in laminar flow [19].

Chapter 3: Development of Methane Condensing Unit

3.1 Proof of Concept: First Generation Condenser

The Methane Condensing Unit (MCU) used to produce liquid methane for the HHFTF has gone through several development iterations. The first generation design was developed as a proof of concept to demonstrate the feasibility of condensing methane at a larger scale, as well as to gain experience handling cryogenics. The first generation condenser was constructed using a vacuum insulated flask; this condenser was able to produce 1 L of LCH_4. The proof of concept condenser was a shell and coiled tube heat exchanger which used LN_2 as the coolant. To estimate the amount of liquid methane that was condensed in the vacuum flask, the dewar was placed on a scale to determine the mass of the condensed methane; furthermore, a type E thermocouple placed inside the flask read the saturation temperature of methane when 1 L of liquid methane had been produced. Figure 3.1 shows the proof of concept condenser.

Figure 3.1: Proof of Concept Condenser Experimental Setup

3.2 Transient Data: Second Generation Condenser

When the proof of concept condenser demonstrated that liquid methane could be successfully produced, a second generation condenser was developed; this condenser system had a capacity of 2 L

and consisted of two separate 304 SS Swagelok tanks. The second generation condenser was developed as a two-tank system due to safety concerns; since one of the tanks had been cut and modified to allow the placement of the condensing coil and instrumentation inside the tank, the 6.9 MPa pressure rating was voided. Figure 3.2 shows the condensing tank fitted with thermocouples and wrapped in insulation.

Figure 3.2: Second Generation Condensing Tank Wrapped in Cryogenic Insulation

To overcome the issue of the voided pressure rating, the condensing process was conducted at pressure of 34 kPa; when the condensing tank was full, a transfer valve was opened, which would transfer the LCH_4 into the run tank placed underneath the condensing tank. However, some liquid methane was lost during the transfer process due to vapor lock venting issues; as a result, the condenser was only able to provide sufficient methane to obtain transient data. Figure 3.3 shows the second generation condenser and an overview of the two-tank system.

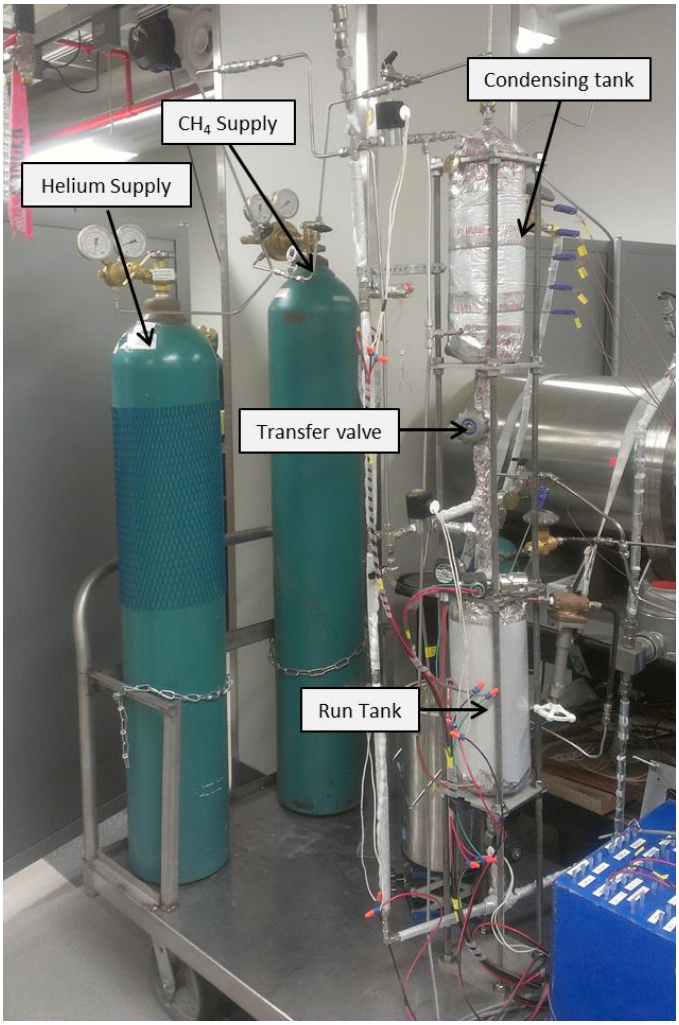

Figure 3.3: Second Generation Condenser System Setup

3.3 Steady State Data: Third Generation Condenser

To be able to perform longer duration tests and obtain steady state subcritical liquid methane cooling data, a third generation condenser Methane Condensation Unit (MCU) was developed. Similar to the second generation condenser that used double ended cylinders as the working tanks, the third generation condenser was developed using a 13 L stainless steel double ended cylinder rated at 3.45 MPa. Due to the tank's pressure rating, the upgraded condenser serves as a run tank at cryogenic temperatures, thus eliminating the transfer process described in the second generation condensing procedure. Furthermore, the single-tank condenser was also fitted with an inner coil to condense the gaseous methane and was wrapped with a copper coil to maintain the tank walls cold, as shown in Figures 3.4 and 3.5, respectively.

Figure 3.4: Inner Coil Used to Condense Gaseous Methane

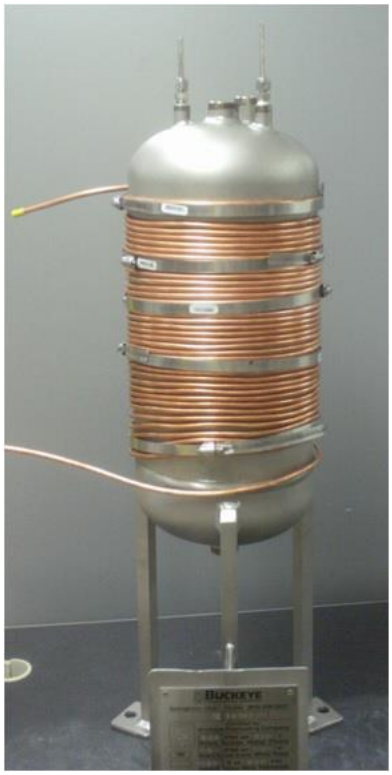

Figure 3.5: Copper Auxiliary Coil Placed Around Tank to Maintain Cold Wall Temperature

Similar to the second generation condenser, the third generation condenser was wrapped with three layers of cryogenic insulation. When compared to the second generation condenser, the third generation MCU was more proficient due to the elimination of the transfer process and shorter condensing times; more specifically, while the second generation condenser would condense approximately two liters in two hours, the third generation MCU was capable of condensing thirteen

liters in approximately ninety minutes due to the higher working pressures that the MCU allows. To check methane temperatures in the tank, eight ungrounded sheathed type E thermocouples are placed inside ports located vertically along the tank. Figure 3.6 shows the whole MCU system integrated with the gaseous methane tank, pressurant (helium), and liquid nitrogen.

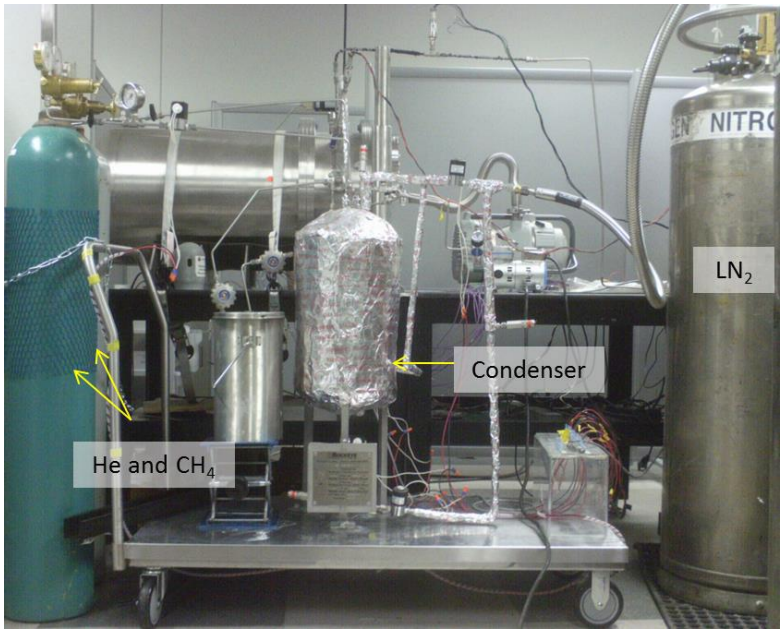

Figure 3.6: MCU Integrated to Coolant and Pressurant

Chapter 4: High Heat Flux Facility

4.1 High Heat Flux Test Facility Technical Approach

The HHFTF was developed to investigate the heat transfer characteristics of LCH_4. A significant portion of the test facility's design was based on the carbothermal rig built by Bates et al due to the advantages of conductive heating over resistive heating [9]. The HHFTF uses a copper block equipped with heating cartridges to provide a conductive hot wall with constant heat flux on which the cooling channel test section is placed. Figure 4.1 shows a model of a test section resting on the copper block.

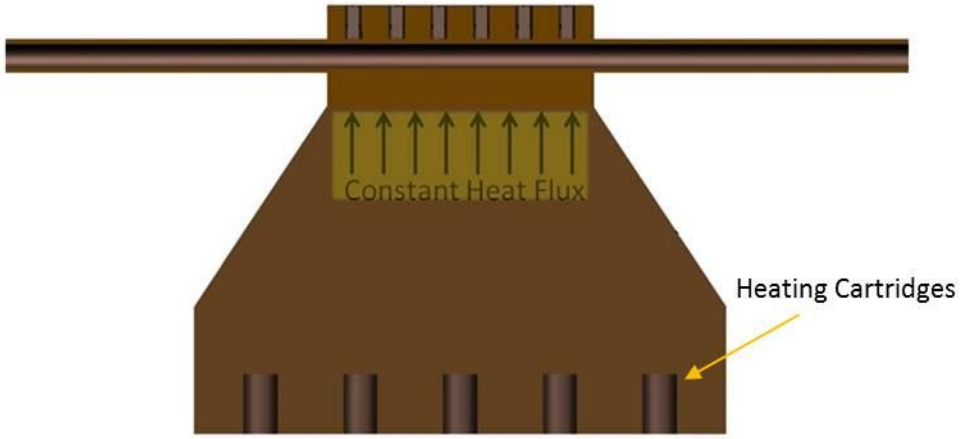

Figure 4.1: Model of Test Section Placement on Heating Block

The conductive heating simulates the conditions that the coolant in a regen engine cooling channel is exposed to. Design requirements considered during the development of the HHFTF include compatibility with LCH_4, and the ability to withstand temperatures as low as -180 °C. Although the HHFTF was influenced by the carbothermal rig described by Bates et al, the HHFTF design was modified to simplify the system. For example, the HHFTF is simpler because it contains no moving parts, and the cooling channel test articles used in the HHFTF are interchangeable; that is, the test sections can be simply removed and replaced with another test article without having to modify the heating block, as was the case with the carbothermal rig developed by Bates et al [5, 9].

4.2 HHFTF Components

The main components that the HHFTF consists of are the stand, cradle, heating block, and test section. The components are installed inside a vacuum chamber to reduce convective heat losses and

reduce oxidation of the components when exposed to high temperatures. Figure 4.2 shows the main components and the vacuum chamber in which the components are placed.

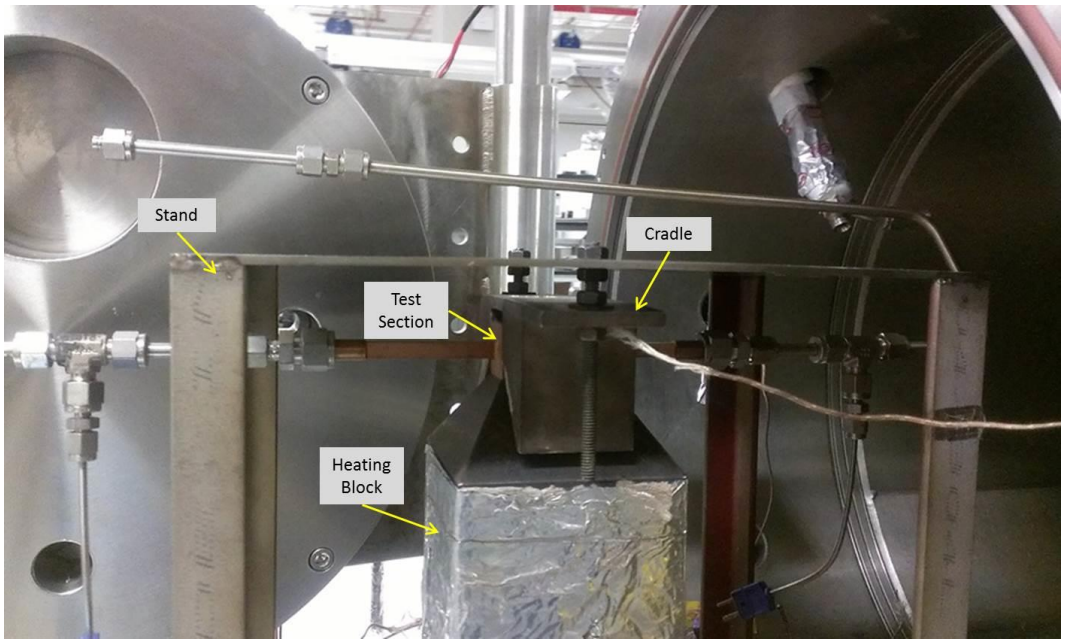

Figure 4.2: High Heat Flux Test Facility Components

4.2.1 Stand

The HHFTF stand supports the heating block and is used to secure the test section and cradle onto the heating block. The stand is constructed of 3.2 mm thick 304 SS plate welded together, and has four L-shaped legs. The block rests on small plates welded onto L-shaped brackets, and a 5 cm by 5 cm cutout is located underneath the block to allow the cartridge heater wiring to be directed towards the vacuum wiring feed through. To secure the cradle onto the test section and block, the top plate has two holes that allow the bolting of the cradle to the stand. Figure 4.3 shows a CAD model of the stand.

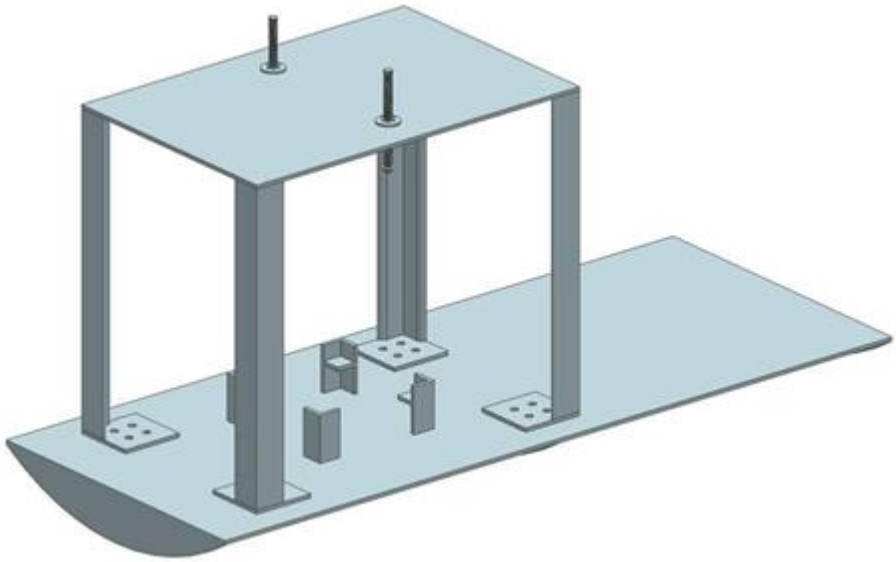

Figure 4.3: CAD Model of Stand

4.2.2 Cradle

The purpose of the cradle is to position the test article in place on top of the heating block. Not only does the cradle hold the test section in place, but it also applies pressure on the test section to provide proper contact between the heating block and the test section. The cradle sits above the test section and heating block and in between the heating block and stand. The cradle has a 3.2 mm wide, 4 cm long opening to allow thermocouples to be placed on the test section cooling channel wall. Aluminum 6061 was used to machine the cradle due to its ease of machinability. To protect the aluminum from the high heating block temperatures, ceramic alumina plates are fitted between the heating block and the cradle. Figure 4.4 shows a model of the cradle.

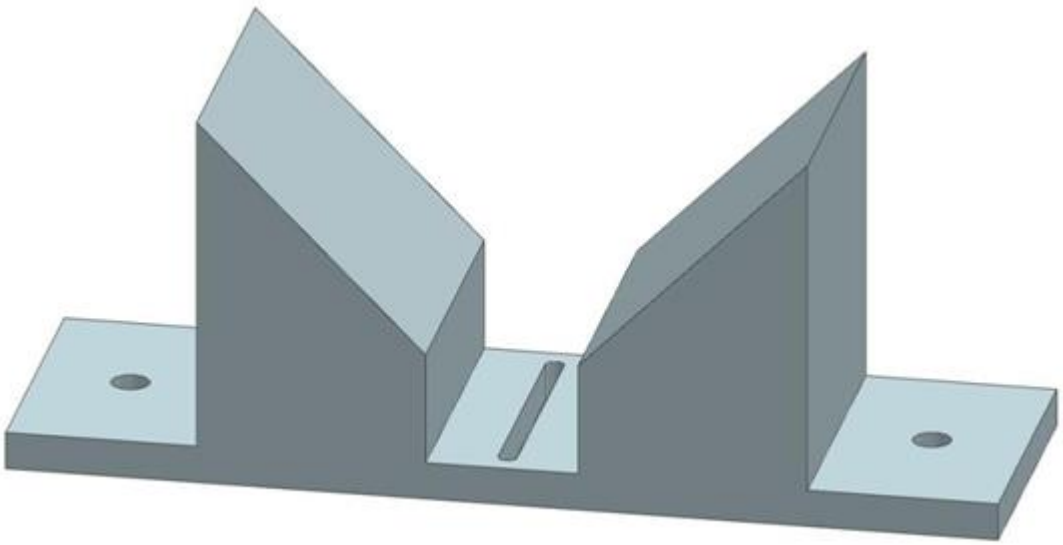

Figure 4.4: CAD Model of Cradle

4.2.3 Heating Block

To provide the test sections with a heat flux, a heating block made of C12200 is used. Copper was selected as the heating block material because of its high thermal conductivity (339 W/m K) [20]. The block dimensions are10.16 x 10.16 x 17.78 cm; the top has taper angles of 45° and 33.7°, and the 10.16 by 10.16 cm cross section reduces to 5.08 x 2.54 cm. The tapered heating block design geometrically focuses the block's thermal energy onto the smaller surface area that the test section is in contact with. Figure 4.5 shows a model of the tapered-top copper heating block.

The heating block temperature is monitored with four type K thermocouples held in place by the cradle. The block has twenty-five 6.4 mm-diameter, 12.7 cm-deep holes that were drilled to house the heating cartridges. Figure 4.6 shows the bottom face of the block, which has the 25 slots for the heaters to be inserted.

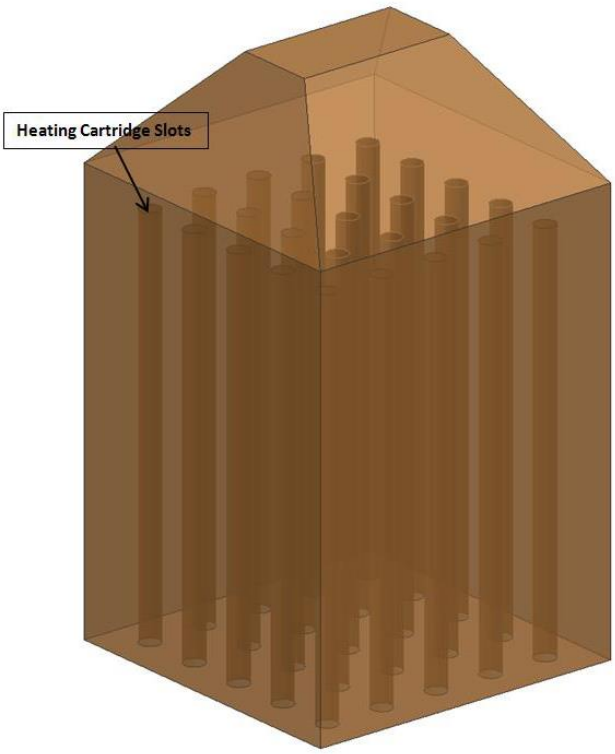

Figure 4.5: CAD Model of Copper Heating Block

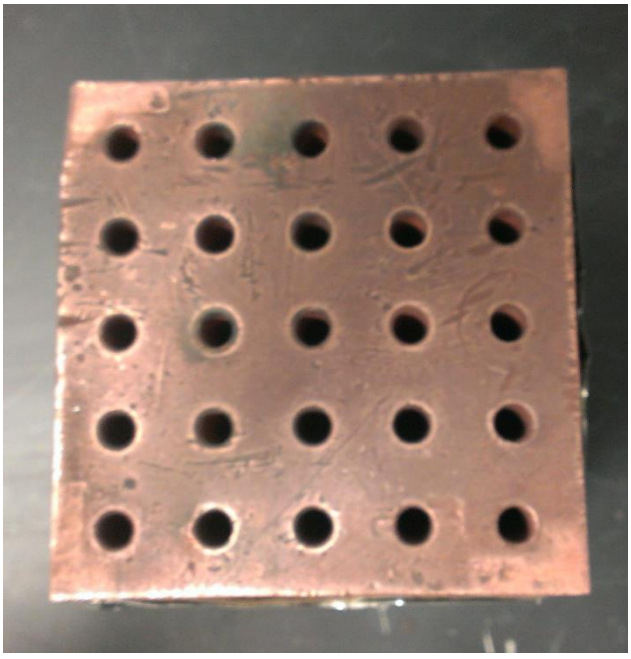

Figure 4.6: Bottom Face of Heating Block with Heating Cartridge Slots

To reduce radiative losses on the heating block's largest faces, the block is wrapped with cloth fiber insulation; aluminum foil is used to secure the insulation on the block. Figure 4.7 shows the heating block wrapped with the cloth fiber insulation and aluminum foil.

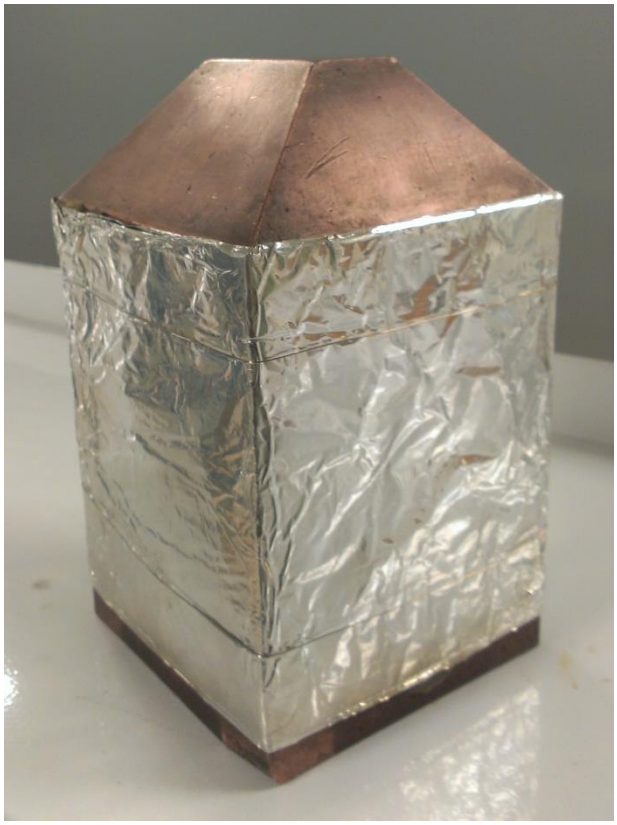

Figure 4.7: Heating Block Insulated with Cloth Fiber

4.2.4 Test Sections

The HHFTF test sections offer a modular design that allows different test sections to be removed and replaced by other test sections with different characteristics without modifying the heating block or other components. Test section traits that can be investigated without major modification include different channel cross-sectional geometries or surface finishes. All test sections share a modular space of 5.08 x 2.54 x 2.54 cm through which the subscale cooling channel passes through. The test sections used in the experiment are made of copper C18200; since other studies investigated the effects of flowing hydrocarbons through copper channels exposed to high heat fluxes, the test sections in the current study are also machined out of copper. Another reason why copper is used in cooling channel studies is because copper is the industry standard for cooling channel wall materials due to copper's

highly conductive thermal properties [21]. The test sections used in the experiment have square cooling channels with a cross section of 3.2 x 3.2 mm. Furthermore, the experiment studied one channel with a smooth surface finish, as well as three additional channels with longitudinal ribs, all of which were machined with electric discharge machining (EDM). With the addition of longitudinal ribs in the cooling channel and maintaining the channel cross-sectional geometry constant, it is expected that the cooling effectiveness will increase at the expense of an increased pressure drop. The longitudinal fin geometries were dictated by machining limitations by fin-to-hydraulic-diameter ratios of 0.1, 0.2, and 0.25, while the cross-sectional geometry was influenced by entry length requirements. To ensure fully developed turbulent flow, the test sections required an entry length of at least 10 hydraulic diameters; the actual entry length of the test sections is 18 hydraulic diameters (5.72 cm) [22]. Figure 4.8 shows a cross sectional view of a test section with the entry length and exit length.

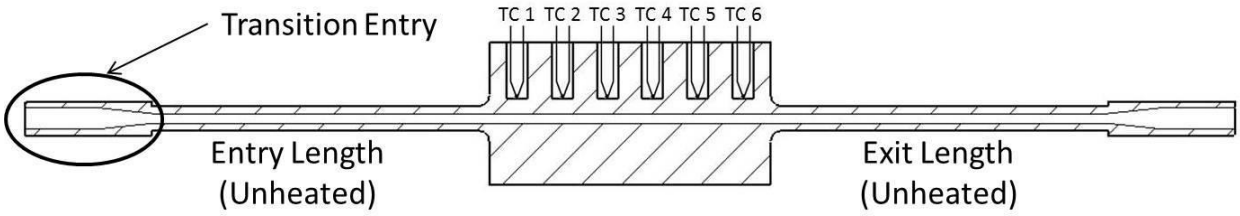

Figure 4.8: Cross Sectional View of Test Section

All test sections have six 3.2 mm diameter thermocouple ports machined along the top face. All ports are 12.7 mm deep to ensure that the thermocouples do not work their way out of the holes, and the channel wall thickness is 1.3 mm. In addition, the thermocouple holes are spaced at a center- to-center distance of 8.1 mm.

Smooth Cooling Channel

The smooth cooling channel was machined with the purpose of providing baseline results to compare the performance of the other channels; namely, the channels with longitudinal fins. The smooth channel is a subscale representation of a single channel milled channel in a regen engine. In addition, the channel is a modification to previous channels that had been developed in a NASA Johnson Space

Center/UTEP collaboration to investigate milled and brazed tube cooling channels. Figure 4.9 shows a view of the smooth cooling channel.

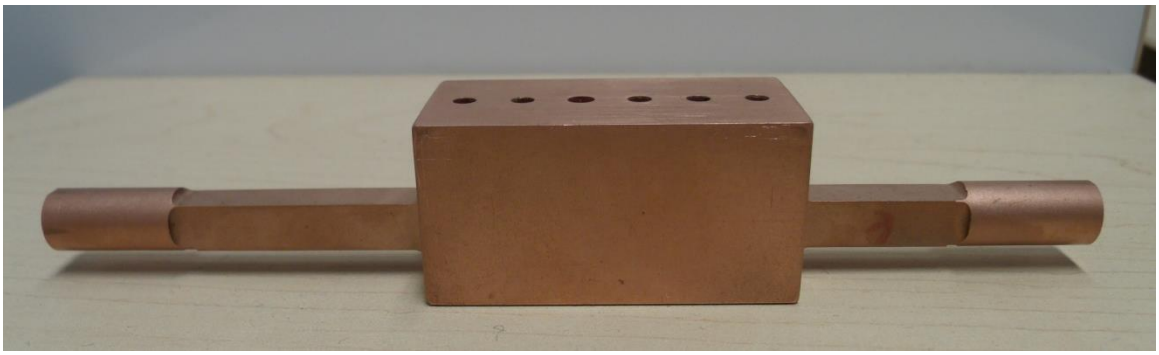

Figure 4.9: Side View of Smooth Cooling Channel (3.2 mm x 3.2 mm Cross Section)

Longitudinally Finned Channels

The longitudinally finned channels were studied to observe the effects of this type of heat transfer enhancement in cooling channels. As previously mentioned, it is expected that maintaining a constant cross-sectional geometry and increasing the fin-to-hydraulic diameter ratios from 0.1, 0.2, and 0.25 will increase cooling effectiveness at the expense of an increased pressure drop. Figure 4.10 shows a view of the longitudinal fins machined in one of the finned cooling channels.

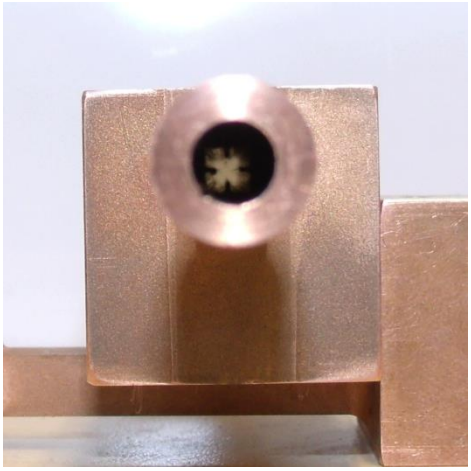

Figure 4.10: Interior View of Finned Cooling Channel

Chapter 5: System Integration and Elements

5.1 System Integration

The HHFTF is used in conjunction with the MCU previously described to obtain steady state subcritical LCH_4 heat transfer characteristics. The two systems are integrated with 316 SS tubing with an outer diameter of 6.4 mm. Figure 5.1 shows a fluid schematic of the integrated systems, namely, the HHFTF and the MCU.

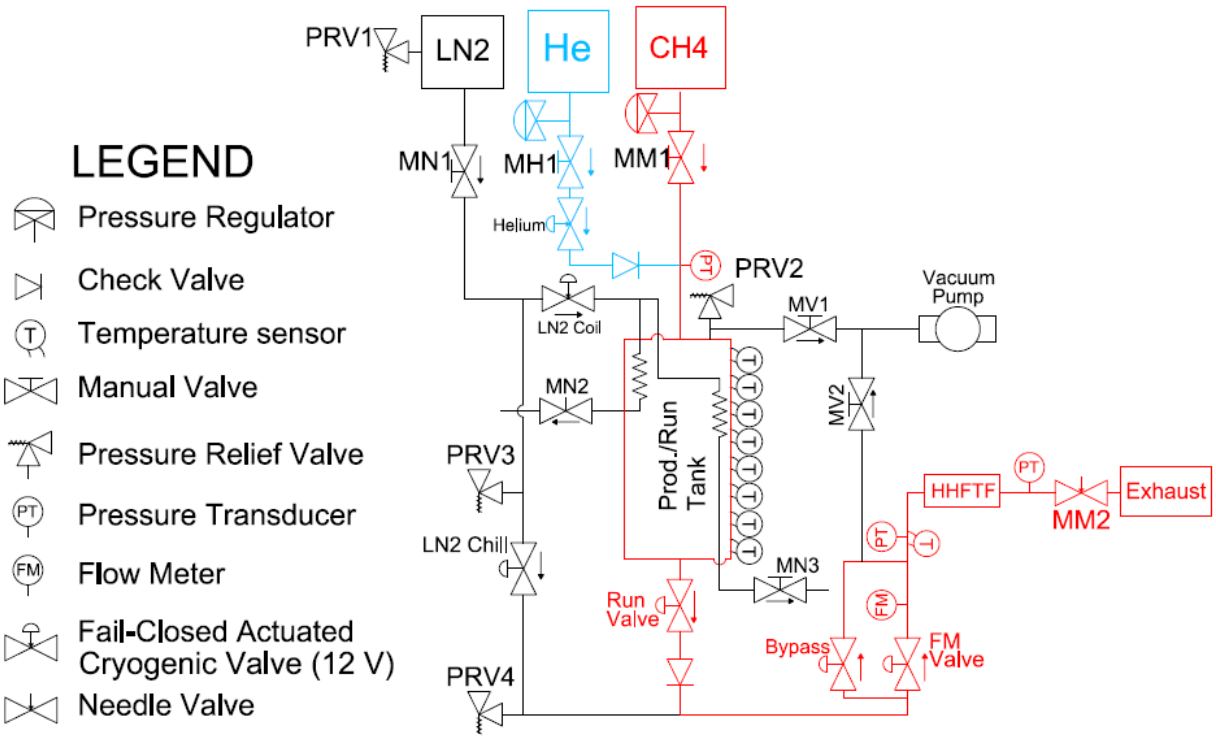

Figure 5.1: Integrated System Fluid Schematic.

Additional testing components in the MCU/HHFTF integration include a cryogenic backpressure needle valve and vacuum pumps. Figure 5.2 shows the integration of the MCU to the HHFTF. Detailed descriptions of additional components will be presented below.

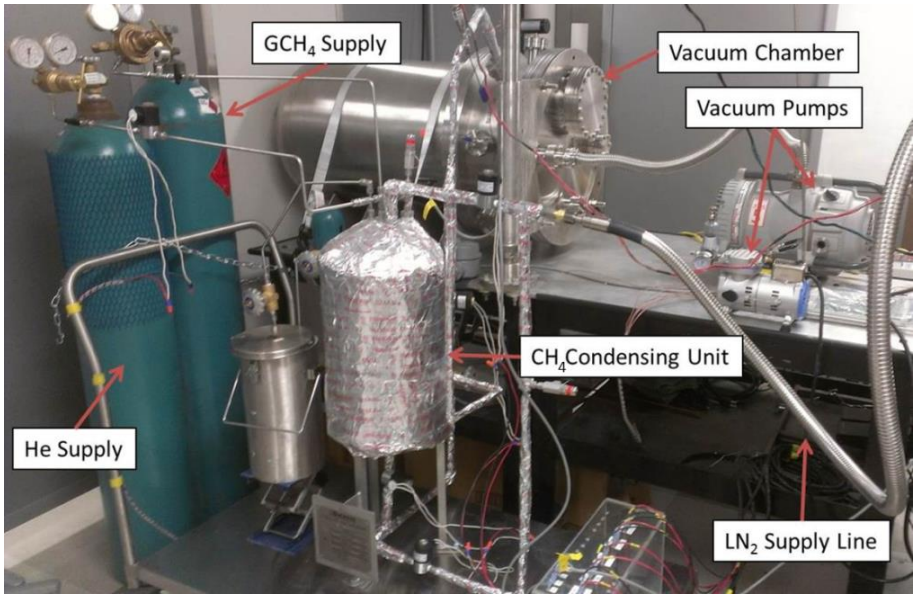

Figure 5.2: Integration of MCU to HHFTF

5.2 Data Acquisition, Flow, Pressure, and Temperature Measurement

The main categories encountered in the experiment that require measurement include mass flow, pressure, and temperature. Due to the nature of the experiment, the components must endure a wide range of temperatures, from cryogenic to the high temperatures (650 °C max) present at the heating block. During a test, the flow, pressure, and temperature are frequently observed, and the DAQ system records data; more specifically, pressures and temperatures are monitored while the MCU is used to condense LCH_4, and flow rates are observed while LCH_4 flows through the test article.

5.2.1 Pressure Measurement

Tank and line pressures are monitored using cryogenic-compatible pressure transducers (PT). The pressure transducers used are 3.45 MPa Omega PX1005L1-500AV Thin Film Cryogenic Pressure Transducers. The pressure transducers have a 30 mVdc full range output and a 10 Vdc excitation voltage input. The accuracy of the cryogenic pressure transducers is 0.25% full scale output with a temperature range of -196 °C to 149 °C. Overall, three pressure transducers are used to measure pressure; one is used to measure tank pressure, and two other pressure transducers are used to measure the pressure at the inlet and exit of the test section. Figure 5.3 shows the Omega pressure transducers used in the experiment.

Figure 5.3: Omega Thin Film Crogenic Pressure Transducer

To power the transducers and filter the pressure transducers' readings, Omega Engineering DIN Process Meters are used. The DIN Process Meters will be further discussed with the HHFTF data acquisition system.

To measure the vacuum level in the vacuum chamber, a Kurt J. Lesker 317 Series Pirani Gauge is used; in addition, an MKS HPS 947 Convection Enhanced Pirani Gauge Controller is used to display the vacuum level within the vacuum chamber. Figure 5.4 shows the Pirani gauge and controller.

a) b)

Figure 5.4: a) KJL 317 Series Pirani Gauge. b) MKS Convection Enhanced Gauge Controller

5.2.2 Temperature Measurement

The experiment uses two types of thermocouples to measure temperature. Eight ungrounded sheathed type E thermocouples are used to measure the temperature of methane in the condensing tank. In addition, six exposed tip type E thermocouples read the test section channel wall temperatures and two ungrounded sheathed type E thermocouples monitor the bulk temperatures. All wetted thermocouples are installed using Swagelok fittings to ensure a leak proof connection. Figure 5.5 shows an example of a wetted thermocouple with a Swagelok fitting.

Figure 5.5: Sheathed Thermocouple with Swagelok Fitting

To measure the temperature of the heating block, four Nextel™ insulated type K thermocouples are used.

5.2.3 Mass Flow Measurement

The flow meter used in the system is a Hoffer HO Series turbine flow meter. The flow meter has a working pressure limit of 41.4 MPa; in addition, it has a linear flow range of 1.32 liters/minute to 13.2 L/min. The flow meter has a shielded, self-lubricating hybrid ceramic ball bearing, and it uses a magnetic pickup coil to transmit flow data. The turbine flow meter has an accuracy and linearity of +/- 0.1% of the measured reading, and has an excitation voltage of 13-30 Vdc. The flow meter is used in conjunction with a turbine flow meter DC transmitter. Figure 5.6 shows the flow meter installed in the HHFTF setup.

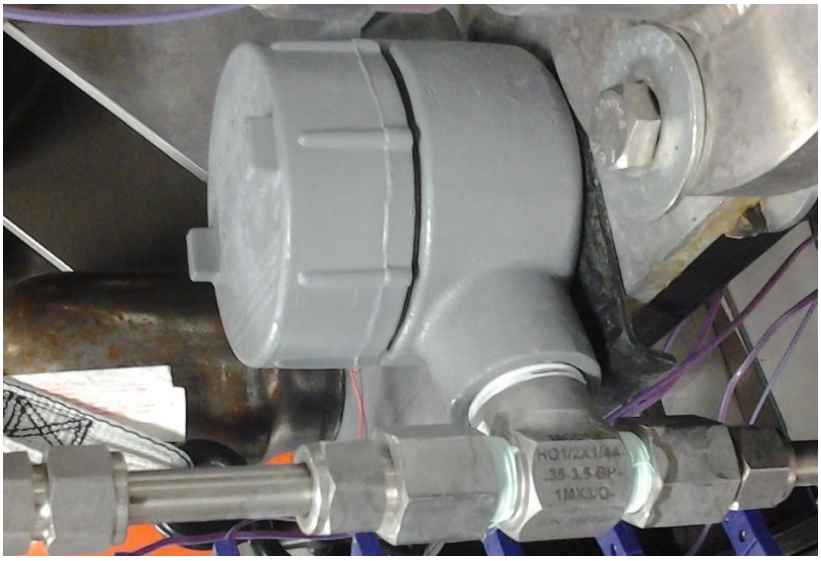

Figure 5.6: Hoffer HO Series Turbine Flow Meter

5.2.4 Data Acquisition System

A data acquisition (DAQ) system is used to monitor the system status while heating the block and condensing methane and to record data when LCH_4 is flowed through the test section. Two NI 9213 sixteen-channel thermocouple input modules are connected to the setup's computer via a USB cable to record condensing tank, heating block, bulk, and test section channel wall temperatures; data is recorded at a rate of 10 hertz. To record pressure data, the pressure transducers are connected to an SCC-68 card that is connected to a NI PCI-6533 card. In addition, the pressure transducers are powered by Omega Engineering DIN Process Meters; the process meters convert the 3 to 30 mV signal to a 0 to 10 V resolution in order for the data acquisition system to record the signal and for a live meter to display the pressures in real time. Figure 5.7 shows the hardware used in by the DAQ system.

Figure 5.7: DAQ hardware: Left to Right: NI PCI-6533, NI SCC-68, NI 9213, DIN Process Meter

5.2.5 Graphical User Interface (GUI)

The HHFTF data is recorded using LabVIEW 13.0 software from National Instruments (NI). The GUI displays real time data from the DAQ system, as shown in Figure 5.8.

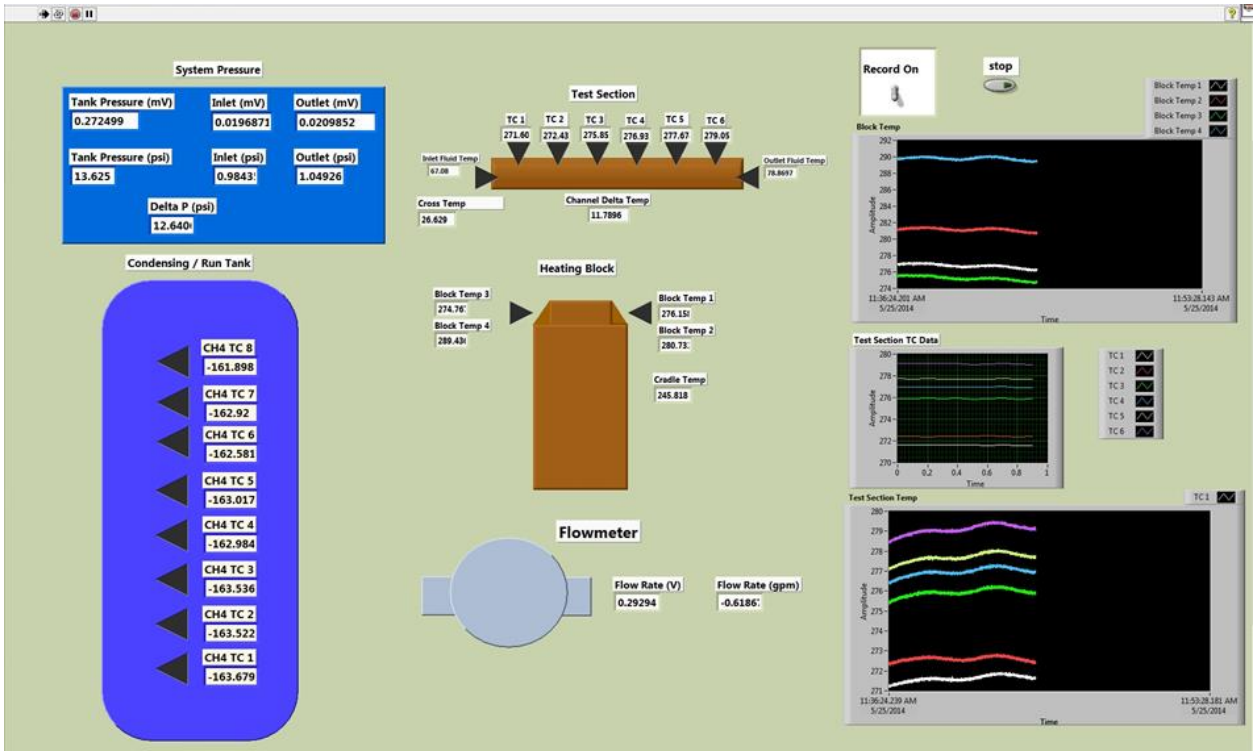

Figure 5.8: NI LabVIEW 13.0 GUI

The GUI was developed to display system pressures, flow rate, condensing tank temperatures, test section wall temperatures, bulk temperatures, and heating block skin temperatures on the front panel. When the system has been prepared and methane is to be flowed through the test section, a switch labeled “Record On” is activated to begin the data recording process. When the methane has been depleted, the switch is flipped, and the data recording process ends.

5.3 System Valves

The HHFTF/MCU setup uses several types of valves; namely, Swagelok quarter turn valves, cryogenic manual valves, actuated cryogenic valves, cryogenic check valves, and pressure relief valves. The quarter turn valves are not rated for cryogenic conditions; therefore, these valves are used only to pressurize the condenser with helium or methane and to hold vacuum in the lines when the pumps are turned off. The quarter turn valves are rated to a pressure of 6.9 MPa and are sized for use with 6.4 mm outer diameter tubing. Figure 5.9 shows a Swagelok quarter-turn valve.

Figure 5.9: Swagelok Quarter-Turn Valve

Another type of valve used in the MCU is a cryogenic hand valve. These valves are brass short stem glove valves manufactured by RegO Products. The cryogenic globe valves have a pressure rating of 4.1 MPa and have female national pipe thread (NPT) connections. These cryogenic globe valves are used to control the flow rate of LN_2 through the MCU's coils. Figure 5.10 shows a RegO cryogenic globe valve.

Figure 5.10: RegO Cryogenic Globe Valve

In addition to the cryogenic globe valves, the system requires a cryogenic needle valve to regulate the system backpressure. The needle valve is placed downstream of the test section, and has a maximum operating pressure of 68.9 MPa at -223 °C. The backpressure valve is made by Dragon Valves Inc. Figure 5.11 shows the backpressure regulating valve.

Figure 5.11: Backpressure Regulating Needle Valve

The MCU is also equipped with cryogenic actuated valves to better control the flow of LN_2 or LCH_4 during a test sequence. More specifically, cryogenic actuated valves are used to allow LN_2 to flow through the MCU's condensing coils, as well as to allow LN_2 to flow into the test section for pre-chilling. Another actuated valve is used to begin the flow of LCH_4 when a test is conducted. The cryogenic actuated valves are D-Cryo Series valves manufactured by Gems Sensor and Controls; these valves have a maximum pressure rating of 2.6 MPa and have a power requirement of 12 Vdc. Figure 5.12 shows an image of the cryogenic solenoid valves.

Figure 5.12: Gems Sensor and Controls D-Cryo Series Actuated Valves

Generant cryogenic check valves are used to prevent LN_2 from flowing into the condenser while the line is being chilled. The poppet type cryogenic check valves have a maximum allowable working

pressure of 20.7 MPa. Also, to prevent pressure buildup from cryogens that could become trapped in the lines, Swagelok pressure relief valves are used. Pressure relief valves are installed on the condenser and in the system line where cryogens could become trapped between two closed valves. Figure 5.13 shows the cryogenic check valves, and Figure 5.14 shows the Swagelok pressure relief valves.

Figure 5.13: Generant Cryogenic Check Valve.

Figure 5.14: Swagelok Pressure Relief Valve.

5.4 Vacuum Pumps

The HHFTF requires two types of vacuum pumps during an experiment. One pump is used to pull vacuum in the condenser and the system lines through which methane will flow; this is done to

remove any trapped moisture within the lines that would freeze when exposed to cryogenic temperatures, which could obstruct the flow of LCH_4 during a test. The other pump is used to pull vacuum in the chamber in which the heating block and test section are placed to reduce convective losses in the chamber and to reduce oxidation of the copper heating block and test section.

The vacuum pump used to pull vacuum in the system lines is a Rocker 300 piston pump. This pump can pull a maximum vacuum of 0.11 Torr at 2 L/minute. Figure 5.15 shows an image of the piston pump.

Figure 5.15: Rocker 300 Vacuum Pump

The vacuum pump used to pull vacuum in the chamber is a XDS5 scroll pump manufactured by Edwards. The Edwards scroll pump is capable of reaching an ultimate vacuum of 4.5 x 10-2 torr at 6.7 m^3/hour. Figure 5.16 shows an image of the scroll pump.

Figure 5.16: Edwards XDS5 Scroll Vacuum Pump

5.5 Electrical Components

The HHFTF requires power from different sources for the electrical components used. For example, alternating current (AC) is used to power heating cartridges, while direct current (DC) is used to provide excitation voltage to pressure transducers or actuated valves. Other power requirements are described below.

The copper heating block is heated using eighteen 120 VAC, 400 W cartridge heaters manufactured by Gordo Sales, Inc. as shown in Figure 5.17. The heaters are controlled using a series of six Omega solid state relays (SSR) rated at 50 A. Only three cartridge heaters are wired per relay to avoid overdrawing current from the laboratory power source; even though the relays are rated at 50 A, the laboratory power source can only provide 20 A. The SSR control voltage requirement is 3 to 30 Vdc, and the relays can be used to supply 24 to 240 Vac at a max current of 50 A; Figure 5.18 shows the Omega SSRs used in the experiment. The SSRs are activated manually by using a switch that connects the SSR to a 5Vdc power source; when the switch is flipped, all relays activate and allow the relays to receive power. A wiring schematic showing the SSR electrical connection is included in the Appendix.

Figure 5.17: Cartridge Heaters Inserted in Heating Block.

Figure 5.18: Omega Solid State Relay

The electrical components that require direct current are powered by two Extech Quad Output DC power supplies, which is shown in Figure 5.19. Components that are connected to the power supply include the previously mentioned actuated valves, flow meter transmitter, and relays.

Figure 5.19: Extech Quad DC Power Supply

5.6 Test Procedure

The test procedure consists of heating the copper block used to subject the test section to a constant heat flux while methane is being condensed. When the methane has condensed, the LCH_4 is flowed through the cooling channel and the data is recorded. A brief overview is presented below; however, a detailed procedure is included in the appendix.

Before beginning a test, the system is checked for leaks by pressurizing the lines and shutting off the pressurant; if the pressure in the lines drops quickly, it is likely that a leak exists in the lines. When

the system is declared leak-free, the instrumentation and equipment are inspected to ensure that taken measurements are correct. An oxygen meter is also turned on and configured to sound an alarm if oxygen levels fall below 18%. After verifying that there are no irregularities in the system lines and instrumentation, the condensation process is begun. The condensation process begins by pulling vacuum in the condensing tank and system lines. At the same time, the vacuum chamber that houses the test section and heating block is evacuated. When the lines have been completely evacuated, the condenser is pressurized with gaseous methane, and LN_2 is flowed through the condenser coils. While the methane condenses, the heating cartridges are manually controlled to raise the heating block's temperature. To help the cartridge heaters last for longer periods of time, the heaters are operated using a three seconds-on three seconds-off cycling method.

When the condensing process has been completed, the run tank is pressurized with helium. As the tank is pressurized, the delivery line is chilled in with LN_2. When the delivery line has been chilled, the backpressure needle valve is set to the appropriate position to obtain the required flow. When the line inlet temperature, run tank pressure, and heating block heat flux are at the required levels as per the test matrix, the DAQ recording system is initiated and the actuated delivery valve is opened so that LCH_4 can flow through the test article and the data can be recorded. When the LCH_4 has been depleted, the system is purged with helium, and then the lines are evacuated by using the piston vacuum pump.

Chapter 6: Results and Discussion

6.1 Test Matrix Development

The tests in the experiment were conducted following a test matrix that specified tank pressure and block temperature. The parameters that were kept constant for the tests include the tank pressures and channel inlet temperature. A channel inlet temperature of approximately -165 °C was achieved by flowing LN_2 through the test article to avoid wasting LCH_4 in cooling the test article and risk not reaching steady state conditions. The tank pressure, which ranged from 1.0 MPa to 2.1 MPa dictated the flow rates and Reynolds number variation for the tests. Flow rates were related to tank-to-inlet pressure difference with a calibration test. Table 6.1 shows the block temperatures and tank pressures for the test matrix developed for the smooth and finned channels.

Table 6.1: Test Matrix developed for the smooth and finned 3.2 mm x 3.2 mm Cooling Channels

Tank Pressure (MPa)	Block Temperature (°C)	
1.03	200	275
1.55	200	275
2.07	200	275

6.2 Flow Rate Calibration

Mass flow rate of LCH_4 during a given test was determined by a calibrated delta-pressure measurement. The flow meter was not used to measure LCH_4 flow rate real-time because use of the turbine flow meter during a test did not permit wall temperatures to reach steady state. This is because a significant amount of LCH_4 is wasted in cooling the flow meter. LN_2 was not used to chill the flow meter because the initial water hammer and cryogenic boil off could damage the flow meter by over-spinning the turbine. The calibration method used dedicated LCH_4 flow rate test cases to measure pressure difference between the tank and the inlet of the test section. This method eliminates the need to perform a calibration test for every test section (i.e., the calibrated pressure drop was not performed across the test article). Tank-to-inlet pressure is varied with a backpressure valve placed downstream of the test article. During a flow rate calibration test, the backpressure valve is opened gradually while LCH_4 is flowed through the test article. Figure 6.1 shows the methane flow rate calibration relating the

mass flow rate to the pressure drop. Density for the LCH_4 was calculated using REFPROP [23], with the state definition at the test article inlet pressure and inlet temperature.

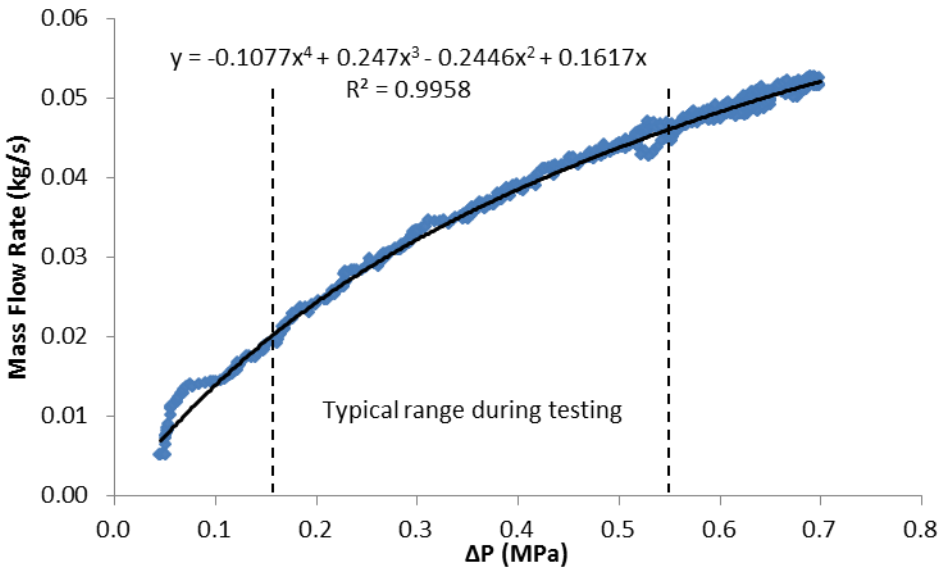

Figure 6.1: Methane Flow Rate Calibration Curve for Pressure Drop from Tank to Test Article Inlet

6.3 Test Section Measurements

Of the measurements recorded during a test, the two primary test section measurements are pressure and temperature; more specifically, the tank, channel inlet, and channel outlet pressures, as well as the channel wall and fluid inlet/outlet temperatures are used to develop the results. Figure 6.2 shows an example of the thermocouple placement on the test section to measure channel wall temperature, T_w. The channel wall temperature is measured with six axially placed type E thermocouples spaced 8.3 mm apart along the length of the channel. Thermocouple-to-channel surface contact is verified by checking continuity between the exposed thermocouple tip and the channel surface by using a multi meter.

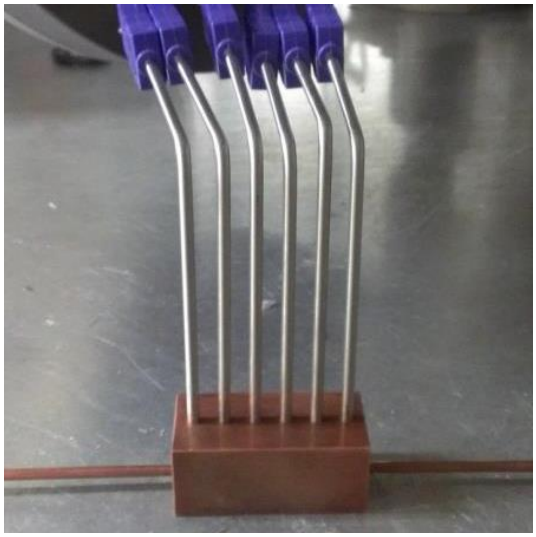

Figure 6.2: Thermocouple Placement on Test Section for Wall Temperature Measurement

The measured wetted fluid temperatures, which are measured with two ungrounded sheathed type E thermocouples, are used calculate the heat flux applied to the single-phase fluid; the heat flux is then used to calculate the heat transfer coefficient. To ensure that the LCH_4 flow was fully developed at the heated section of the test article, the channel inlet wetted thermocouple was installed before an entry length of ten hydraulic diameters. Figure 6.3 shows an illustration of the channel wall and wetted thermocouples placement on the cooling channel. The analysis also depends on the pressures at the channel inlet and outlet. Pressure transducers are located at the tank, at the channel inlet, and channel outlet; it should be noted that the transducers are placed outside of the vacuum chamber. The fluid properties are evaluated at the bulk temperature and average pressure due to the relatively large difference in wall and bulk temperature [24].

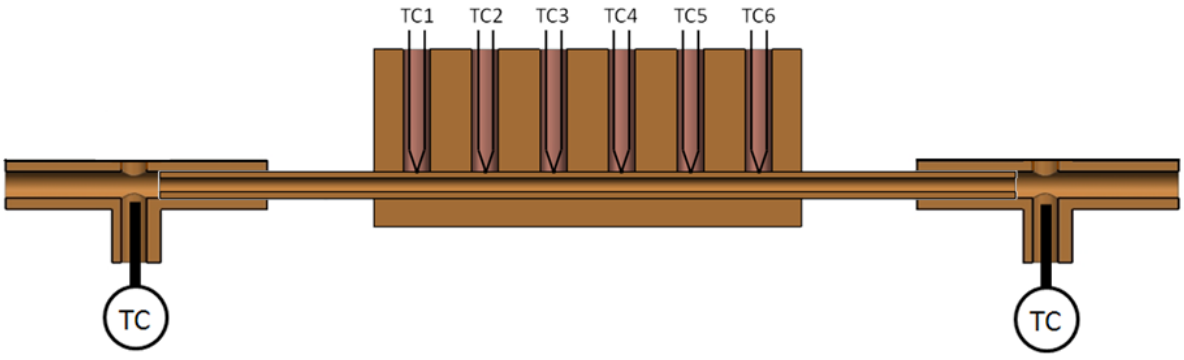

Figure 6.3: Channel Wall and Wetted Thermocouple Placement on Test Section

6.4 Data Analysis

An objective of the current study was to develop correlations for Nusselt number, *Nu*, and Reynolds number, *Re*. Total rate of heat transfer to the fluid was calculated based on the mass flow rate of the fluid, fluid, $\dot{m}$, specific heat, *Cp*, and temperature change from fluid inlet to outlet, ΔT, as in Eq. (6.1) [22]. Surface heat flux, $\dot{q}_s$, was determined using the test section coolant channel wall surface area, A_s, as in Eq. (6.2).

$$\dot{Q} = \dot{m} C_p \Delta T \tag{6.1}$$

$$\dot{q}_s = \frac{\dot{Q}}{A_s} \tag{6.2}$$

Mass flow rate, $\dot{m}$, was determined from the pressure-drop calibration for mass flow rate (described above). The resultant heat flux is then used to calculate the local heat transfer coefficient, h_x, shown in Eq. (6.3),

$$h_x = \dot{q}_s / (T_s - T_m) \tag{6.3}$$

where T_m is the mean fluid temperature and is calculated using Eq. (6.4).

$$T_m = T_{in} + \frac{\dot{q}_s p}{\dot{m} C_p} x \tag{6.4}$$

T_{in} is the channel inlet fluid temperature, p is the perimeter of the tube, and x is the axial location along the heated segment of the cooling channel. With h_x, an average heat transfer coefficient h_L was calculated using Eq. (6.5).

$$h_L = \frac{1}{L} \int h_x dx \tag{6.5}$$

The measured Nu_L is then calculated using Eq. (6.6) where k is the fluid thermal conductivity.

$$Nu_L = \frac{h_L D_h}{k} \tag{6.6}$$

Shown in Eq. (6.7), bulk Reynolds number was defined using the fluid density, ρ, fluid viscosity, μ, test article hydraulic diameter, D_h, and bulk velocity, v, which is calculated from the $\dot{m}$, ρ, and cooling channel cross sectional area.

$$Re = \frac{\rho v D_h}{\mu} \tag{6.7}$$

All the state properties such as ρ, μ, Cp, and k, were calculated with REFPROP [23] at the average fluid pressure, P_{avg}, where $P_{avg} = ½ (P_{in} + P_{out})$, and bulk temperature, T_b, where $T_b = ½ (T_{in} + T_{out})$. T_{out} is the fluid temperature at the channel outlet.

6.4.1 Measurement Uncertainty

The determination of the maximum uncertainty for the data points collected pertains mainly to accuracies of the components reported by the vendors. Using Table 6.2, which shows the error associated with each parameter, the propagation of uncertainty shown in Eq. (6.8) is used to find the combined error for each parameter. This error is the resultant effect for the measured quantities from the flow meter, temperature, and pressures. The error in mass flow rate measurement is directly influenced by the flow meter during the calibration tests and the resultant pressure differential relationship attained during the actual LCH_4 test runs. Similarly, the heat transfer coefficient error stems from the temperature measurements associated with the channel wall and fluid thermocouples. The fluid state properties are evaluated using REFPROP [23] which includes an accuracy of ±0.2 that also affects mass flow rate. Taking into account these values, the combined uncertainty for Nu_L is estimated to be +/- 6.2%.

$$(U_{cal.}) = \sqrt{\sum \left(\frac{\partial f(Calculated)}{\partial Variable} Error_{variable} \right)^2} \tag{6.8}$$

Table 6.2: Measurement Accuracy Associated for Each Component

Parameter	Error %
Turbine Flow Meter	± 0.10
Pressure Transducers	± 0.25
Thermocouples	± 1.00
REFPROP (Fluid Properties)	± 0.20
Pressure Differential	± 0.35
Temperature Differential	± 1.40
Mass Flow Rate	± 1.23
Local Heat Transfer Coefficient	± 2.42
Measured Nusselt Number	± 6.20

6.5 Steady State Data

The steady state data analysis only considers the portion of the test in which wall and bulk temperatures are steady state. Figure 6.4 shows an example of a test performed with the 3.2 mm x 3.2 mm channel with 0.8 mm high fins. "TC 1" through "TC 6" in Figure 6.4 refers to the channel wall temperature measurements; "TC1" is the temperature measurement closest to the channel inlet, and "TC 6" is closest to the outlet of the channel. "Inlet" and "Outlet" refer to the methane temperature at the inlet and outlet of the test article, respectively. The test shown in Figure 6.4 was initiated at approximately Time = 3 s. A ten second steady-state interval is defined for all temperature measurements in each test. The steady-state interval begins at approximately Time = 245 s for the test shown in Figure 6.4. Methane is depleted approximately 260 seconds into the test, as indicated by the red dashed line.

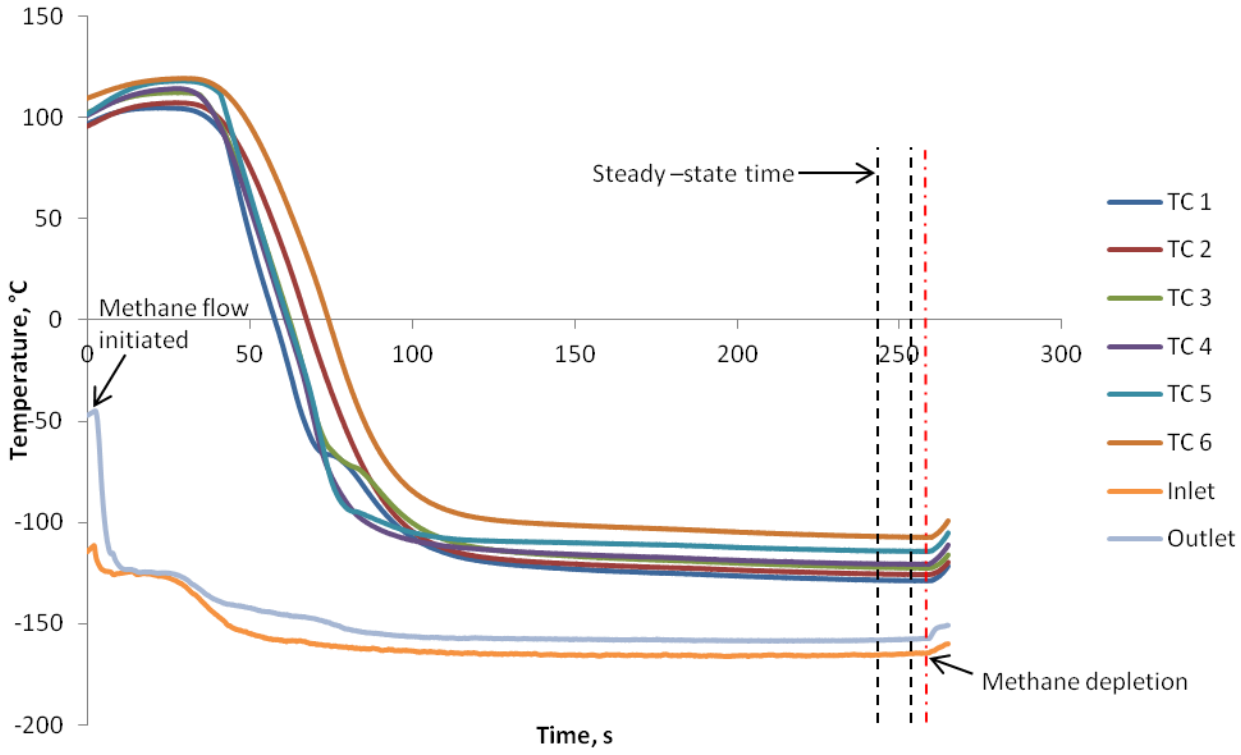

Figure 6.4: Steady State Temperature Profile, 3.2 mm x 3.2 mm, Finned Channel

6.5.1 Smooth and Finned Channels, 3.2 mm x 3.2 mm

For the cooling channels presented in this study, 24 data points were obtained. Figure 6.5 shows example test measurements of the six T_w thermocouples and fluid temperatures for the smooth 3.2 mm x

3.2 mm channel. Note that the "Steady-state" time is when the wall temperatures are averaged for the data points. Figure 6.6 shows example test measurements of the T_w thermocouples and fluid temperatures for the 3.2 mm x 3.2 mm channel with the 0.8 mm high fins.

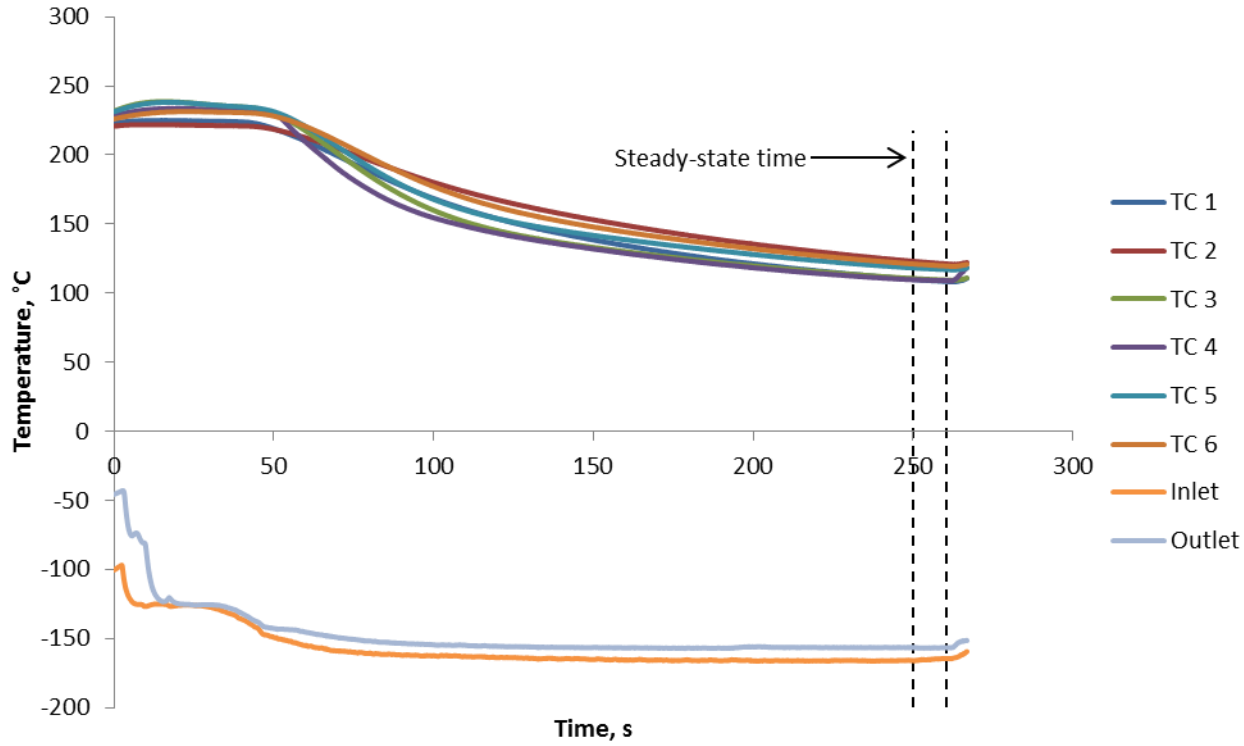

Figure 6.5: Example Test Measurements of the Six T_w Thermocouples and Fluid Temperatures as a Function of Time, Hot-Wall Test, 3.2 mm x 3.2 mm Smooth Test Article

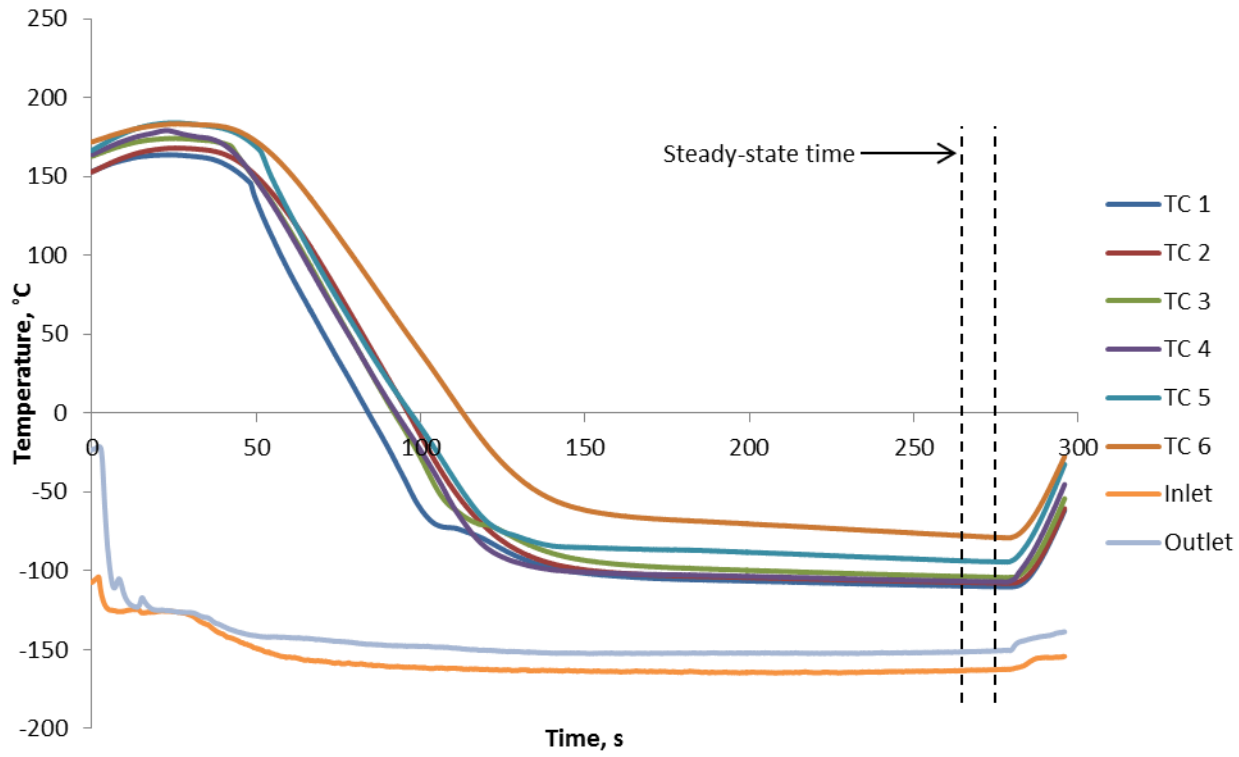

Figure 6.6: Example Test Measurements of the Six T_w Thermocouples and Fluid Temperatures as a Function of Time, Cold-Wall Test, 3.2 mm x 3.2 mm Test Article with 0.8 mm High Fins

The steady state measured Nusselt number versus bulk Reynolds number plot is shown in Figure 6.7. This figure shows that the range of Nusselt numbers is between 70 and 510 and Reynolds numbers range between 50,000 and 128,000. The data points showed that in some tests, the channel wall was cooled more effectively than others; that is, in some tests, the channel wall temperatures were below 0 °C. Figure 6.5 shows an example of a "hot-wall" test and Figure 6.6 shows an example of a "cold-wall" test. The data was classified in two categories; namely, hot-wall, and cold-wall. Cold-wall denotes the data where all channel wall temperatures were below 0 °C, while hot-wall denotes the data points in which all channel wall temperatures were above 0 °C. The differences between hot-wall data and cold-wall measurements suggested that there could be a film-boiling phenomenon in the data. Since these experiments were all conducted with LCH_4 that had been cooled with LN_2, the inlet condition to the test article was always sub-cooled. Any film-boiling phenomenon measured in the test article would be classified as "sub-cooled film-boiling". The Nusselt numbers represent the convective component of the

heat flux, as calculated by Eq. (6.1) and Eq. (6.2) (i.e., heat used in boiling is not measured or included in the *Nu* term).

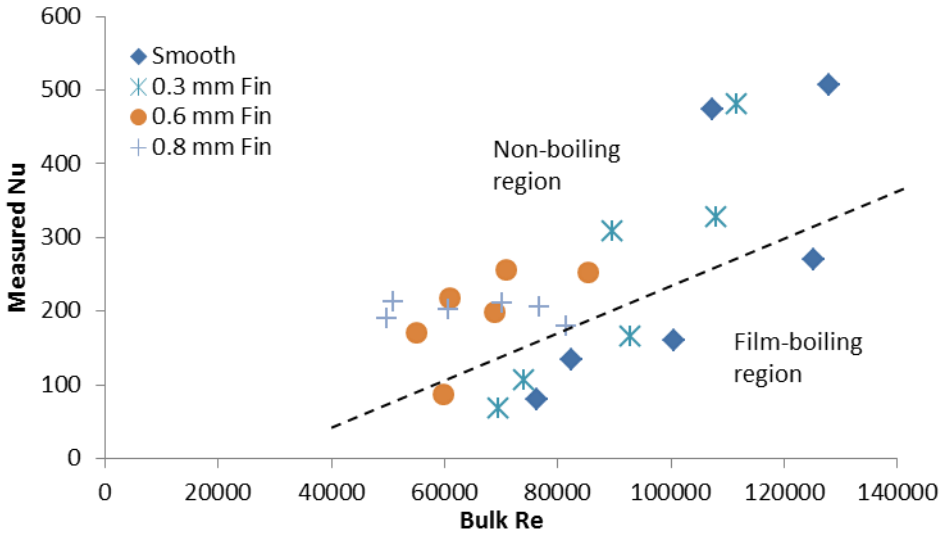

Figure 6.7: Measured Nusselt Number as a Function of Bulk Reynolds Number, 3.2 mm x 3.2 mm Test Articles with Fins

Figure 6.8 shows the heat flux versus average wall temperature minus saturation temperature where the modes of heat transfer can be observed; more specifically, the non-boiling and film-boiling regions. In the film-boiling regime, all six thermocouples in T_w measurement read "hot" together, indicating that the critical heat flux (CHF) onset occurs in the 5.1 mm prior to the first wall thermocouple. It should be noted that the smooth channel had four data points in the film-boiling regime, while the finned channels had more data points in the non-boiling region. In other words, boiling phenomena was also present in the finned channel data; however, the quantity of film-boiling tests was fewer. It should be noted that the heat flux values were calculated using the conservation of energy equation for the steady flow of a fluid in a tube as in Eq. (6.1). This equation is only valid for the convective heat transfer; however, it is used as an approximation of the actual heat fluxes of the film-boiling data. The apparent reduction in heat flux at higher wall temperatures is a result of more heat going into the boiling than into raising the bulk temperature of the fluid.

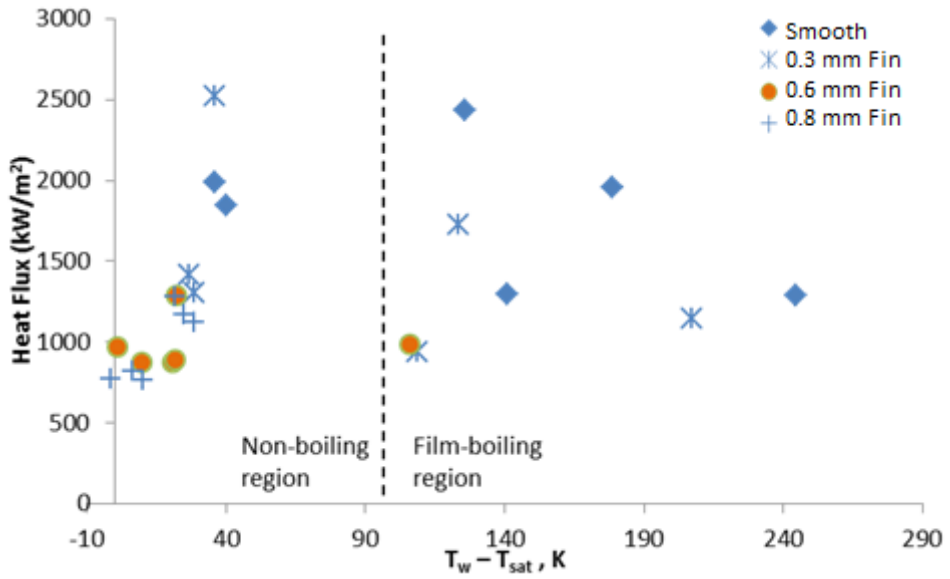

Figure 6.8: Heat Flux as a Function of Average Wall Temperature Minus Saturation Temperature, (T_w-T_{sat}), 3.2 mm x 3.2 mm Test Articles with Fins

As shown in Figure 6.8, the measured CHF for the onset of sub-cooled film-boiling appears to be ~2000 kW/m^2 at velocities ranging from ~6 to 11 m/s, though the distinction for the CHF is not obvious. For comparison, Van Noord reported CHF at ~2000 kW/m^2 at low velocities (~15 m/s) and up to ~5000 kW/m^2 at higher velocities [10]. Also, previous studies of methane reported CHF in the ~300-1300 kW/m^2, scaling with $v^{0.9}$ [11].

As noted above, a range of velocities were studied (note all velocities are shown in Figure 6.8). In order to normalize the different data points for the variable velocities, a Boiling Number, *Bo*, was used. The boiling number is defined as the ratio of the critical heat flux, $\dot{q}_{sCHF}$, to the CH_4 heat of vaporization, i_{fg}, and mass flow per channel cross-sectional area, A_c. For this study, all data points were calculated for *Bo* at the measured $\dot{q}_s$ (shown in Eq. 6), in order analyze $\dot{q}_s$ for CHF.

$$Bo = \frac{\dot{q}_s A_c}{i_{fg}\dot{m}} \tag{6.9}$$

Figure 6.9 shows the boiling number, *Bo*, vs. ΔT (T_w-T_{sat}), where T_{sat} refers to the saturation temperature. From this figure, it can be observed that the critical heat flux occurs at a *Bo* value of approximately 0.1.

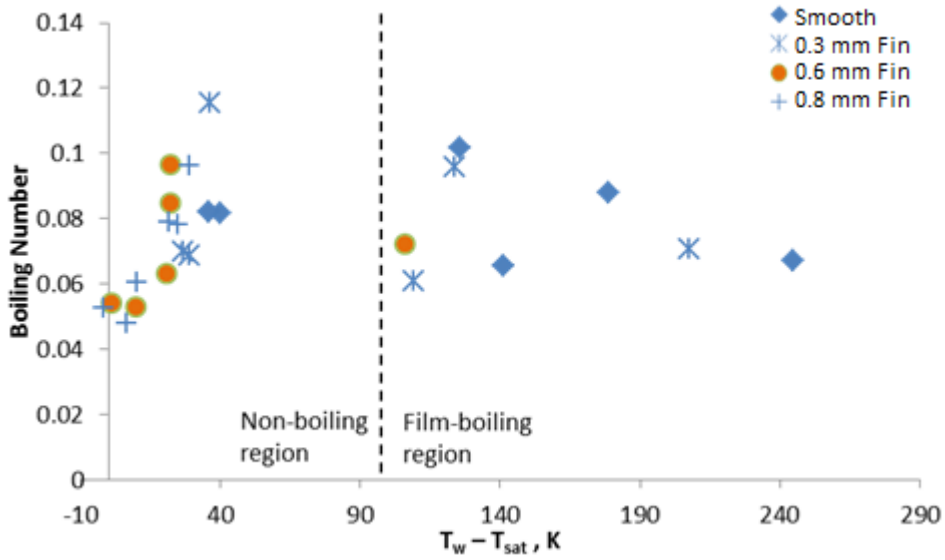

Figure 6.9: Boiling Number as a Function of Average Wall Temperature Minus Saturation Temperature, (T_w-T_{sat}), 3.2 mm x 3.2 mm Test Articles with Fins

This value of *Bo* ~0.1 matches well with the Shah correlation for CHF in tube flow, described in [25]. In the Shah "upstream conditions correlation", *Bo* is related to a critical length of tube, z_{crit}, needed to reach CHF for a given amount of sub-cooling (i.e., negative quality, x) in the upstream conditions. Other state properties and geometric parameters are considered in the Shah correlation, but the *Bo* prediction is simplified here for the attention to the primary factors of (z_{crit}/D_{hyd}) and $(1-x)$. In this study, the data points around the measured CHF had sub-cooled quality x ~ -1.2 to -1.4. It is assumed that the CHF occurs before the first wall thermocouple position, which indicates (z_{crit}/D_{hyd}) ~2. Based on inspection of the Shah "upstream conditions correlation" plotted in [25], the predicted *Bo* would be ~0.1.

In 1984, Cook conducted an experimental investigation in which a Nusselt number correlation for supercritical CH_4 flowing through smooth channels was developed. Cook's correlation included a temperature correction factor based on a T_b to T_w ratio [7]. Huzel and Huang also presented a temperature correction factor based on a T_b to T_w ratio which is described for "heat transferred through a vapor film boundary layer" for supercritical propellants [3]. Since heat is being transferred through a vapor film boundary layer in the sub-cooled film-boiling cases, the temperature correction factor was used. Figure 6.10 shows the measured Nusselt number versus the predicted Nusselt number based on

Cook's correlation. Recall that the measured Nusselt number only includes the convective component of the heat transfer. Since the temperature correction factor accounts for the heat transferred through a vapor film boundary layer, the film-boiling data lines up well with the single-phase range when the T_b/T_w correction factor was used [7]. Note that the data scatter in the "cold-wall" single phase test data points is much broader than the "hot-wall" film-boiling points, and analysis of this data scatter is in work. It should also be noted that data scatter may be explained by the corrected surface area, A_s, and hydraulic diameter, D_{hyd} of the finned channels.

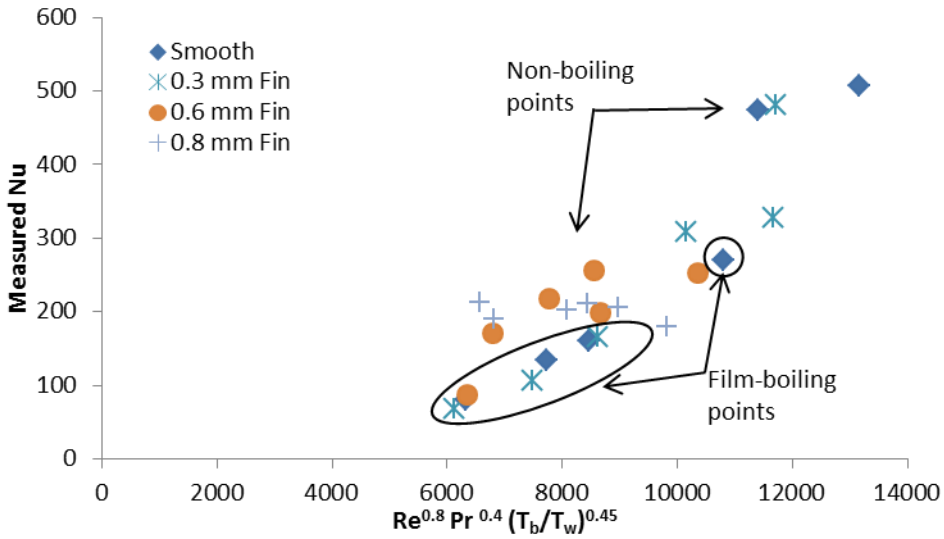

Figure 6.10. Measured Nusselt Number as a Function of Predicted Nusselt Number Based on Cook's Correlation [7], 3.2 mm x 3.2 mm Test Articles with Fins

Chapter 7: Conclusion

7.1 Conclusion

The smooth cooling channel tested is a valid representation of a cooling channel in a regen engine. The finned channels are based on regen engine cooling channels, but were modified to study the heat transfer enhancement of longitudinal fins. A total of 24 steady-state tests were completed with the smooth and finned channels to study the heat transfer characteristics of LCH_4 and compare the cooling performance of the smooth and finned channels. The results presented below were obtained from the experiments in the study.

Sub-cooled film-boiling phenomena were discovered in the data pertaining to the smooth and finned channels with heights of 0.3 mm and 0.6 mm. The finned channel with 0.6 mm high fins only had one data point in which boiling was present; sub-cooled film-boiling was not observed in the finned channel with 0.8 mm high fins. For all the channels, the critical heat flux appears to occur at a boiling number value of approximately 0.1. This value matches well with the Shah upstream conditions correlation for CHF in tube flow [25].

A Nusselt number correlation with a temperature correction factor based on a bulk temperature to wall temperature ratio that takes into account the heat transferred to a vapor film boundary layer was used for all channels [3, 7]. The correlation showed to work well for the film-boiling regime.

For the 3.2 mm x 3.2 mm channels presented in this study, the measured critical heat flux for the onset of sub-cooled film-boiling appears to be 2000 kW/m^2 at velocities ranging from 6.2 to 11.3 m/s, though the distinction of the CHF is not obvious; the result is comparable to the data presented by Van Noord [10].

For the longitudinally finned channels, Nusselt numbers were lower than the smooth channel Nusselt numbers. However, the lower Nusselt numbers obtained for the channels with longitudinal fins can be explained by the increase in surface area that the fins provide. Moreover, the finned channels had fewer data points in which film-boiling was present. As mentioned before, to better characterize the finned channels, more data points are needed.

7.2 Future Work

An analysis to determine the total heat flux in the the film-boiling regime should be conducted to fully characterize the heat transfer characteristics of two-phase methane. Furthermore, the data scatter in the single-phase regime when applying the Nusselt number correlation presented in reference [7] should be analyzed. To better characterize the effects of longitudinal fins in cooling channels, more testing is required. In addition, more testing is needed to determine the critical heat flux for the range of velocities tested.

References

[1] Neill, T. Judd, D. Veith, E. and Rousar, D. 2009. Practical Uses of Liquid Methane in Rocket Engine Applications. Acta Astronautica, Vol. 65, pp. 696-705.

[2] Younglove, B. A. and Ely, J. F. 1987. Thermophysical Properties of Fluids. II. Methane, Ethane, Propane, Isobutane, and Normal Butane. Journal of Physical and Chemical Reference Data Vol. 16, pp. 577–798.

[3] Huzel, D. and Huang, D. 1992. Modern Engineering for Design of Liquid-propellant Rocket Engines, Volume 147, American Institute of Aeronautics and Astronautics, Washington, D.C.

[4] Morehead, R. L. 2011. Project Morpheus Main Engine Development and Preliminary Flight Testing. 47th AIAA Joint Propulsion Conference Atlanta, AIAA 2011-5927, San Diego, CA.

[5] Bates, R. W. Mass, E. D. Irvine, S. A. and Auyeung, T. P. 2004. Design of a High Heat Flux Facility for Thermal Stability Testing of Advanced Hydrocarbon Fuels. Air Force Research Laboratory, F04611-99-C-0025, Edwards AFB, CA.

[6] Bates, R. W. Edwards, T. and Meyer, M. L. 2004. Heat Transfer and Deposition Behavior of Hydrocarbon Rocket Fuels. Air Force Research Laboratory. AFRL-PR-ED-TP-2002-320, Edwards AFB, CA.

[7] Cook, R.T. 1984. Methane Heat Transfer Investigation. NASA Marshall Space Flight Center, NASA-CR-171199, Huntsville, AL.

[8] Hongfang, G. Hongzhi, L. Haijun, W. and Yushuan, L. 2013. Experimental Investigation on the Convective Heat Transfer from a Horizontal Miniature Tube to Methane at Supercritical Pressures. Applied Thermal Engineering, Vol. 58, pp. 490-498.

[9] Mass, E. Irvine S. A. Bates, R. and Auyeung T. 2004. A High Heat Flux Facility Design for Testing of Advanced Hydrocarbon Fuel Thermal Stability. Air Force Research Laboratory, 4847, Edwards AFB, CA.

[10] Van Noord, J. 2010. A Heat Transfer Investigation of Liquid and Two-Phase Methane. NASA Glenn Research Center, NASA/TM-2010-216918, Cleveland, OH.

[11] Glickstein, M. R. and Whitesides, R. H. 1967. Forced-Convection Nucleate and Film Boiling of Several Aliphatic Hydrocarbons, ASME-AIChE Heat Transfer Conference and Exhibit, Seattle, WA.

[12] Gage, M. L. and Rosenberg, S. D. 1990. Hydrocarbon Fuel/Combustion-Chamber-Liner Materials Compatibility. NASA Lewis Research Center. NASA CR-185203, Cleveland, OH.

[13] Bates, R.W., Billingsley, M.C., and Lyu, H.Y. 2007. Experimental and Numerical Investigation of RP-2 Under High heat Fluxes. Air Force Research Laboratory, AFRL-PR-ED-TP-2007-150, Edwards AFB, CA.

[14] Billingsley, M. 2008. Thermal Stability and Heat Transfer Characteristics of RP-2. Air Force Research Laboratory. AFRL-RZ-ED-TP-2008-259, Edwards AFB, CA.

[15] Green, J. M. Pease, G. M. Meyer, M. L. 1995. A Heated Tube Facility for Rocket Coolant Channel Research. NASA Lewis Research Center, NASA/TM-106968, Cleveland, OH.

[16] Garcia, C. P. 2013. Pressure and Heat Flux Effects on the Heat Transfer Characteristics of Liquid Methane. PhD Dissertation, University of Texas at El Paso, ProQuest/UMI. (Publication No. AAI365907.)

[17] Klimenko, V. V. 1990. A Generalized Correlation for Two-Phase Forced Flow Heat Transfer-Second Assessment. Int. J. of Heat and Mass Transfer, Vol. 33, No. 10, pp. 2073-2088.

[18] Trejo, A. 2014. An Experimental Investigation of the Cooling Channel Geometry Effects on the Internal Forced Convection of Liquid Methane. PhD Dissertation, University of Texas at El Paso, ProQuest/UMI.

[19] Dewan, A. Mahanta, P. Sumithra, K. Suresh P. 2004. Review of Passive Heat Transfer Augmentation Techniques. Proc. Instn Mech. Engrs Vol. 218 Part A: J. Power and Energy.

[20] Young, H. D. Zemansky, M. W. and Sears, F. W. 1987. University Physics. 7th ed., Addison-Wesley, Table 15-5.

[21] Irvine S. A., and Burns R. M. 2005. Preliminary Heat Transfer Characteristics of RP-2 Fuel as Tested in the High Heat Flux Facility. Air Force Research Laboratory, AFRL-PR-ED-TP-2005-545, Edwards AFB, CA.

[22] Cengel, Y.A. 2007. Heat and Mass Transfer. 3rd ed., McGraw-Hill, p. 459.

[23] Lemmon, E. W. Huber, M. L. McLinden, M. O. 2013. NIST Standard Reference Database 23: Reference Fluid Thermodynamic and Transport Properties-REFPROP, Version 9.1, National Institute of Standards and Technology, Standard Reference Data Program, Gaithersburg.

[24] Kreith, F., 2000. The CRC Handbook of Thermal Engineering, Boca Raton: CRC Press LLC.

[25] Collier, J. G. and Thome, J. R. 1996. Convective Boiling and Condensation, 3rd edition, Oxford Science Publications, Oxford.

Appendix

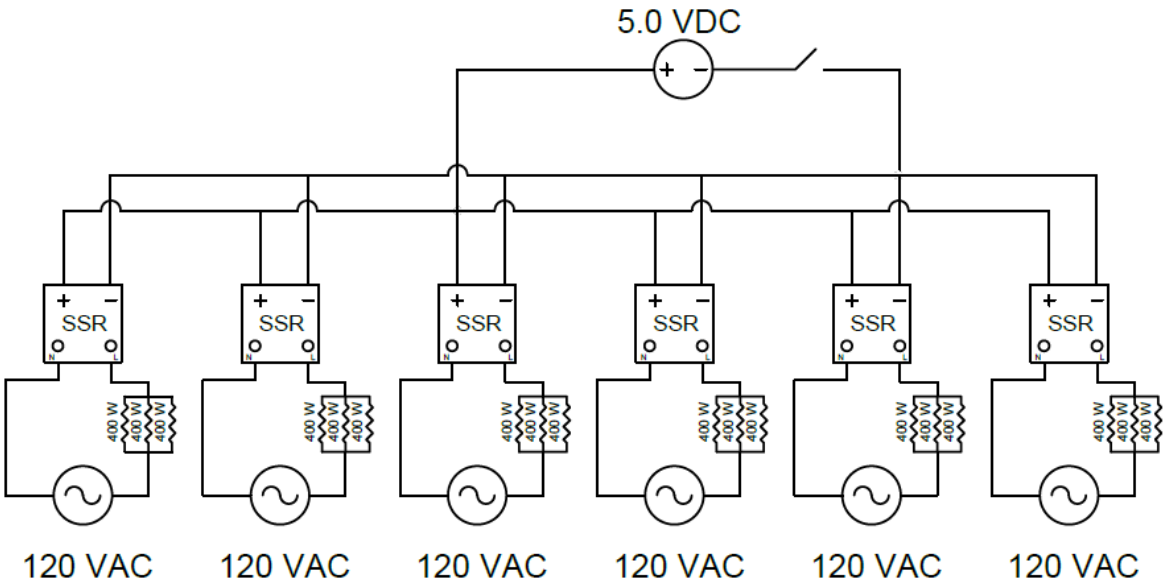

Solid State Relay and Cartridge Heater Wiring Schematic

Detailed List of Instrumentation Used in the MCU-HHFTF System

Item	Make	Model	Range	Accuracy	Use	Quantity
Exposed tip type E thermocouple	Omega Engineering	EMQSS -125E-6	-200 to 900°C (-328 to 1652°F)	1.7°C or 0.5% above 0°C, 1.7°C or 1.0% below 0°C	Test section wall temperature measurement	6
Sheathed ungrounded type E thermocouple	Omega Engineering	EMQSS -125U-6	-200 to 900°C (-328 to 1652°F)	1.7°C or 0.5% above 0°C, 1.7°C or 1.0% below 0°C	Test section inlet/outlet and condenser temperature measurement	8
Nextel ceramic insulated type K thermocouple	Omega Engineering	XC-14-K-12	-200 to 1250°C (-328 to 2282°F)	2.2°C or 0.75% above 0°C, 2.2°C or 2.0% below 0°C	Block temperature measurement	4
Thin Film Cryogenic Pressure	Omega Engineering	PX1005 L-500AV	0 to 3.45 MPa (0 to 500 psia)	±0.25%	Condensing/run tank and test section	3

Transducer			-196 to 149°C (-320 to 300°F)		inlet/outlet pressure measurement	
Thermocouple Input Module DAQ device	National Instruments	NI 9213	Refer manual	Refer manual	Thermocouple data acquisition	2
Terminal Block with SCC Expansion Slots DAQ device	National Instruments	NI SCC-68	Refer manual	Refer manual	Pressure transducer and flow meter data acquisition	1
Turbine flow meter DC transmitter	Hoffer Flow Controls, Inc.	CAT3155DCX1X	-40 to 85°C	±0.02% of full scale @ 20°C (68°F)	Turbine flow meter data transmission	1
Pressure transducer process meter and controller	Omega Engineering	DP25B-E-A	0 to 100 mV	±0.02% of reading	Pressure transducer signal conditioning	3
Convection-enhanced Pirani Sensor	Kurt J Lesker	K31714S	1×10^{-3} to 1.0×10^{3} Torr (1.9×10^{-5} to 19 psi)	±<1%	Vacuum chamber pressure measurement	1
Digital Convection Pirani Vacuum Gauge Controller	MKS	HPS 947	1.0×10^{-3} to 1.0×10^{3} Torr (1.9×10^{-5} to 19 psi)	±<1%	Vacuum chamber pressure digital reading	1

Detailed Experimental Procedure and Safety Hazard/Risk Mitigation Assessment
Pre-testing procedure:

1. Inspect instrumentation and equipment.
    a. Turn on power supplies and adjust required voltage.
        i. Actuated valves: 12 VDC.
        ii. Flow meter transmitter: 13-30 VDC.
        iii. SSRs: 5 VDC.
    b. Run the LabVIEW program titled "High Heat Flux Test Facility" located in the "LabVIEW programs" folder in the computer's desktop.
        i. Ensure that LabVIEW program outputs the data file into a folder titled "Methane Test Data" in the computer's desktop.
    c. Ensure that all pressure transducers and thermocouples are reading ambient conditions (13 ± 1 psia and 23 ± 3°C).
    d. Check that all solenoid valves indicated in the schematic function properly by performing an audible and current draw inspection.
        i. Current draw: 1.2 ± 0.1 A.
    e. Connect solid state relays to 120 VAC extension cords.
    f. Using a multi-meter, check that all cartridge heaters work properly by measuring the resistance across them.
        i. Resistance per group of three cartridge heaters is 12 ± 1 ohms.

2. Inspect testing area.
    a. Activate the ventilation system by turning on the ventilation fans.
    b. Check for leaks in the system using snoop liquid leak detector by pressurizing the lines with He to 50 ± 5 psia.
        i. After leak check is performed close He tank valve and vent system
    c. Close needle valve.
    d. Open MV2 valve and pull vacuum in the system with the line vacuum pump.
        i. Line vacuum levels: 2 ± 1 psia.
    e. Activate and configure oxygen monitor and flammable gas detector devices.
        i. Refer to Appendix A for configuration procedures.
    f. Close line vacuum chamber.
    g. Activate the pirani vacuum gauge controller.
    h. Pull vacuum inside the chamber with the chamber vacuum pump.
        i. Chamber vacuum levels: 0.05 ± 0.01 Torr.

3. Prepare for data collection.
    a. Create a folder in the "Methane Test Data" folder that entails the conditions to be tested i.e. heat flux and pressure.

4. Begin methane condensation.
    a. Turn off the line vacuum pump and close MV2 valve.
    b. Open CH_4 tank valve.
    c. Open MM1 valve.
    d. Put on cryogenic personal protective equipment (PPE), e.g., gloves, apron, face shield.
    e. Pressurize condensing/run tank to 70 psia.

f. Open MN1 valve and regulate dewar pressure to 150 psig.
g. Open LN_2 coil solenoid valve.
h. Open MN2 and MN3 valves.
i. Monitor LCH_4 levels using the tank thermocouples.
    i. At 70 psia, methane is liquid at -139°C.
    ii. Tank is filled with LCH_4 in 60 ± 15 min.
    iii. Please note that the condensing process and the block heating process should occur concurrently.
j. Close CH_4 tank valve.

5. Begin heating the copper block.
    a. Manually activate cartridge heaters by following a 3 sec on/off cycle.
        i. Use manual switch located on the switch panel.
    b. Heat the block until desired conditions are reached.
        i. Stop cycling manual switch.
        ii. Refer to test matrix for testing conditions.

Testing procedure:

1. Chill cooling channel and run lines with LN_2.
    c. Open LN_2 chill and Bypass solenoid valves.
    d. Open needle valve.
    e. Chill until inlet conditions are reached (-160 ± 5°C).
        i. Please note that chilling and pressurizing run tank occur concurrently.
    f. Close needle valve.

2. Pressurize run tank with helium.
    a. Open He tank valve.
    b. Open MH1 valve.
    c. Open Helium solenoid valve.
    d. Pressurize run tank to desired conditions.
        i. Refer to test matrix for testing conditions.

3. Stop LN_2 flow and adjust needle valve.
    a. Close MN1 valve.
    b. Close LN_2 coil and LN_2 chill solenoid valves.
    c. Open and adjust needle valve.

4. Begin data recording process.
    a. Flip “Record On” switch to on position on the GUI.

5. Run LCH_4 through run lines and cooling channel.
    a. Open Run solenoid valve.
    b. Monitor channel wall and tank temperatures.
        i. Tank temperatures warmer than -150°C indicate depletion of LCH_4.
        ii. Observe wall temperature profile in GUI to determine if steady state behavior is reached.
        iii. Channel wall temperature steady state behavior indicates successful test.

c. Close MH1 valve when LCH_4 is depleted.
d. Close Run solenoid valve and needle valve.

6. Stop data recording process.
    a. Flip "Record On" switch to off position on the GUI.

Post-testing procedure:

1. Close He tank valve.

2. Relieve residual system pressure.
    a. Open run solenoid valve.
    b. Gradually open needle valve.
    c. Check that all manual and solenoid valves are open to prevent pressure build up from residual fluids.
    d. Monitor system until ambient conditions are reached.

3. Deactivate all electronic devices.
    a. Turn off chamber vacuum pump.
    b. Check cartridge heaters' resistance to test functionality.
    c. Disconnect solid state relays from 120 VAC extension cords.
    d. Turn off power supplies.
    e. Turn off oxygen meter and flammable gas detector devices.

4. Check that data was collected and transfer it for processing.
    a. Data is used to find the heat transfer coefficient of methane and derive Nusselt number correlations.

Emergency Procedure

All safety considerations were taken and an emergency procedure was developed in case of an unwanted occurrence. Red lines are shown below to avoid a catastrophic failure of the hardware or facilities.

Red Lines:

- Line pressure must remain less than 350 psia.
- Methane tank pressure must remain less than 500 psia.
- Block temperature must remain less than 500°C.

Risks and Hazards:

Hazard	Risk	Mitigation
Cryogenics	Cold contact burns, explosion (pressure), asphyxiation	Cryogenic PPE, pressure relief valves, oxygen monitor device
Flammability	Burns, explosion (ignition)	Fire extinguisher, dilution of LCH_4

Vita

Manuel de Jesús Galván attended the University of Texas at El Paso starting the fall of 2008 and graduated with a Bachelor of Science degree in Mechanical Engineering in the fall of 2011. He started working at the Center for Space Exploration Technology Research in the fall of 2011 as an undergraduate researcher. He then continued his education in the spring of 2012 to pursue a Master of Science in Mechanical Engineering. In the fall of 2012, he interned at NASA Johnson Space Center and worked on the development of a partial regeneratively-cooled lander class engine. His research focus while pursuing his master's involved heat transfer applied to internal forced convection of liquid methane and its applications to regeneratively-cooled engines.

Permanent address: 4732 Sun Valley Dr.
El Paso, TX 79924

This thesis/dissertation was typed by Manuel de Jesús Galván.